Heliyon 10 (2024) e39576

Contents lists available at ScienceDirect

Heliyon

journal homepage: www.cell.com/heliyon

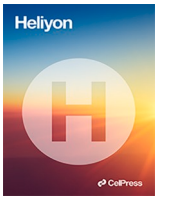

Research article

Thermal and catalytic pyrolysis of automotive plastic wastes to diesel range fuel

Elly Olomo [a,d], Stephen Talai [a], Joseph Kiplagat [a], Egide Manirambona [b,*], Anthony Muliwa [c], Jasper Okino [a]

[a] Department of Mechanical, Production and Energy Engineering, Moi University, P.O. Box 3900 -30100, Eldoret, Kenya
[b] Department of Electromechanical Engineering, Faculty of Engineering Sciences, University of Burundi, Bujumbura, Burundi
[c] Department of Chemical and Process Engineering, Moi University, P.O Box 3900-30100, Eldoret, Kenya
[d] Department of Mechanical Engineering, Faculty of Engineering and Applied Sciences, Uganda Martyrs University, Fort Portal, Uganda

ARTICLE INFO

Keywords:
Pyrolysis
Automotive plastic waste
Calcium bentonite

ABSTRACT

This study investigated the pyrolysis of automotive plastic wastes (APW) for the production of diesel-grade oil products using a modified calcium bentonite clay catalyst. The research aimed to optimize the process for maximum oil yield and diesel range organics yield. The APW was characterized by its chemical composition and physical properties and the optimal temperature and catalyst amount were determined for maximum oil yield and diesel range hydrocarbons. The results showed that the APW contained mixed Acrylonitrile Butadiene Styrene (ABS), High/Low Density Polyethylene (H/LDPE), Polypropylene (PP), Polystrene (PS) and fiberglass, with a large quantity of volatiles and ash. The average oil yield was higher in the catalytic process compared to that in the thermal process. Generally, higher temperature above 450 °*C* produced waxy oil, thus lower temperature favoured more Diesel Range Organics (DRO). Both processes yield similar yields of C_8–C_{24} DRO, and in both cases, lower temperature favoured high yield of C_8-C_{24} hydrocarbons. The catalyst significantly increased the yield of oil, but did not significantly increase C_8–C_{24} DRO yield. The optimal conditions for a maximum oil yield of 78.6 % and DRO yield of 79.5 % was a temperature of 416 °*C* and 24.3 wt% clay. Thus, the modified calcium bentonite clay can be used to improve oil yield from pyrolysis of APW. The oil produced had properties such as calorific value (49.85 MJ/kg), flash point (113 °*C*) and total aromatics 3.55 area%, similar to those of commercial diesel, and comprised mostly of 2,4-Dimethyl-1-heptene (25.37 ± 2.01 %) of thermal and 2, 4 – Dimethyl – 1 – heptane (23.44 ± 2.42) in the catalytic process. The study suggests further research to explore different catalysts, maximization of both DRO and gasoline range organics, recover energy from residues, and conduct techno-economic assessments for plant-scale operations. Additionally, policies on the management of end-of-life vehicles should include provisions for stripping and segregation of plastic components by accredited providers for the purpose of plastics recycling.

1. Introduction

Plastics are important groups of materials that are used in numerous products in modern day to day life. Plastics use has grown

* Corresponding author.
E-mail addresses: egimanm@gmail.com, egide.manirambona@ub.edu.bi (E. Manirambona).

https://doi.org/10.1016/j.heliyon.2024.e39576
Received 11 June 2024; Received in revised form 13 October 2024; Accepted 17 October 2024
Available online 18 October 2024

Nomenclature

α: Mass conversion ratio
area%: Peak area as a percentage of total area
C6 – C10: Organic compounds having 6 to 10 carbon atoms
C9– C20: Organic compounds having 9 to 20 carbon atoms
C8 – C24: Organic compounds having 8 to 24 carbon atoms
C25+: Organic compounds having 25 or more carbon atoms
Wt%: Weight percentage

progressively from the 1950s at a faster rate than any other material, and is expected to double in twenty years [1,2]. Vehicle manufacture is one area that will experience significant growth in use of plastics and other polymer composites [3–6]. This is because plastics contribute substantially to enhanced automobile design, weight reduction, fuel efficiency, safety, and sustainability [6]. Presently, mid-range cars contain 10–15 % plastics, or about 130 kg/vehicle, and with exponential growth in use, automotive plastics will reach 4.88 million tonnes in 2030 [7]. The increased use of plastics, coupled with poor waste management practices have led to the growing problem of plastics pollution world over [8,9], warranting solutions to ensure sustainability of plastics use going into the future.

Recycling plastics from end-of-life vehicles is one of the key measures in the waste hierarchy that ensure sustainable plastic use in a circular economy [4,6,10,11]. Several policy directions and advisory that encourage recycling have been developed, among them the Directive of the European Union Parliament 2000/53/EC on end-of life vehicles, and this is geared toward enhancement of the circular economy.

Recycling through pyrolysis to recover fuels and chemicals has been proposed as suitable method by several researchers such as Cabalová [12] who noted that LDPE, HDPE and PP automotive components can be converted to valuable chemicals in high yields, Netsch et al. [13], who demonstrated the potential of in-situ catalytic pyrolysis recycling of polyolefin-rich plastic to light olefins, and others [14–16]. There has also been strong interest by automotive manufacturers such as Audi who established a partnership with Karlsruhe Institute of Technology to investigate industrial scale automotive plastic recycling [17]. Most studies on automotive plastics focuses on shredder residues that contains mixed polymers, metals and textiles, thus limited information exists on characterizing and recycling of automotive plastic wastes (APW) retrieved from end-of-life vehicles (ELV). While studies on consumer plastics show their suitability for recycling by pyrolysis to suitable liquid fuels such as gasoline as done by Ref. [18]. APW pyrolysis may be challenging due the presence of mineral fillers, flame-retardants, and other additives [19], similar to other engineering plastics.

According to Čabalová et al. [12], APW derived from plastic components including dashboards, bumper, interior panels, headlamps, wheel hubs and others showed suitability for recycling by pyrolysis due to their high volatile content, relatively low decomposition temperature of 375 °C–480 °C, relatively high caloric values of 26.261–45.245 MJ/kg, and production of organic compounds that include those found in gasoline and diesel fuels. Studies on APW pyrolysis show relatively high yield of oil and diesel and gasoline organics. These studies include [20] which resulted in an average yield of 60.44 % from feedstock containing various mixtures of ABS, PP, and PE between 300 °C to 600 °C, and contained organics ethylbenzene, hexene, styrene, heptene, benzene, cyclohexane, and cyclooctatetraene. According to Maqsood et al. [21], HDPE, LDPE, PP, and PS are preferred for pyrolysis. Particularly, PE, and PP produce oil with greater paraffins and olefins, and negligible aromatic compounds are thus preferable for diesel and gasoline type oil [22], while PS yields higher fractions of aromatic compounds [23]. Studies on potential industrial scale recycling show that economic feasibility is still limited by challenges of two kinds mainly, those reacted to feedstock, that is quality and availability, and those related to pyrolysis products quality [24]. These warrant further investigation of APW pyrolysis to establish their yields and composition under various feedstocks and process conditions to provide data to guide process, technological, and policy development to ensure economically feasible and environmentally sound recycling.

In the era of adoption of circular economy concepts, the management of plastic wastes has become a notable global issue, and this has extended to include plastics from end-of-life vehicles [24,25]. Debate on imported plastic wastes have focused on recycled polymers from single use plastics [26]. However, the fact that most countries outside of the Organization for Economic Co - operation and Development, particularly in Sub–Saharan Africa are net importers of used vehicles from the developed economies, especially light duty vehicles which have been shown to last less than 20 years on the road [3], implies that there is an aspect of imported end of life vehicle plastics burden. Thus, the recycling of plastics from end-of-life vehicles may be more urgent that it is assumed in those countries. It is therefore imperative that steps are taken toward ensuring complete recycling of automobiles in line with the aspiration of a global circular economy. This is particularly important since in most developing countries, recycling is not yet wholly adopted, yet are expected to have the highest growth in waste generation.

Catalysts play a crucial role in plastic pyrolysis. They enhance process efficiency [27], product selectivity [28,29], and reduce process temperature and time [30–32] and all these in turn improves cost-effectiveness. While the use of catalysts has been dominated by commercial zeolite catalysts, clay-based catalysts have gained attention due to their low cost and effectiveness, and similar to other acid catalysts, the activity of a catalyst is primarily determined by its surface acidity and pore characteristics, particularly the specific surface area [33]. These properties favour the production of liquid products over gas, with surface acidity facilitating reaction mechanisms through proton addition or hydride ion formation [34,35]. In this regard, modified clay catalysts, such as calcium bentonite [36], kaolin [37], and pillared clays [29,34,38] have shown promising results. Some of the desirable properties exhibited by

pillared clays include relatively high specific surface area, high exchange capacity, low permeability, swelling ability, relatively good heat-resistance stability, high acidic properties, tunable acidity, and relatively low price [38,39]. Fe, Ti, and Zr pillared clays have demonstrated significant improvements in liquid yield or selectivity compared to thermal cracking [40,41]. Particularly, Fe -pillared clays are reported to improve yield and selectivity for diesel-range organics from pyrolysis of PP and HDPE due to suitably large pore sizes and mild acidity [29,38]. Additionally, they are also reported to be less likely to lead to over cracking and hence high gas yields. As such, Fe – pillared clays are top candidates when the goal is to enhance oil and Diesel Range Organics yield without using conventional and commercial catalysts.

This study aimed to establish the characteristics and compositions of plastics from ELV, the yield of oil from their pyrolysis and the composition of the oil. Since Iron-pillared clays, in particular, have been effective in enhancing oil and diesel fraction yields [42] using mixed plastic wastes and thus potentially providing a feasible alternative to conventional commercial catalysts like zeolites, this study used calcium bentonite clay was used as a catalyst as recommended by various researchers as reported by Fadillah et al. [43]. Additionally, the clay was modified by pillaring with iron to assess whether it could indeed improve the selectivity of oil yield with respect to diesel range organic (DRO) compounds. Previous studies had shown that iron pillared clay catalysts show improved selectivity for diesel fractions.

Recycling of automotive plastics is necessary to ensure complete recycling of automobiles in line with the aspiration of a global circular economy. This is particularly important in developing countries where recycling is not yet wholly adopted, yet are expected to have the highest growth in light duty vehicles [44], and associated wastes when those vehicles reach end of life. This would enhance sustainable waste management [12,24,45,46], and the fuel products obtain can also substitute or complement petroleum fuels which are usually imported in most countries, further enhancing energy security, while also reducing environmental pollution.

2. Materials and methods

The overall study methodology is summarized schematically in Fig. 1. The procedure involved the sampling, preparation and characterization of APW feedstock, activation and characterization of calcium bentonite clay, thermal and catalytic pyrolysis process for production of APW pyrolysis oil, and subsequent characterization of the oil with consideration of its physical and chemical properties.

2.1. Sampling and characterization of plastics from end-of-life vehicles

APW was collected from a scrap yard in Asis, Eldoret Municipality in Kenya. The samples were manually sorted by component, cut, washed, sundried then crushed to reduced highest dimensions to 6.30–4.75 mm. The polymer types were determined by Fourier Transform Infrared Spectroscopy (using a JASCO Model FT/IR – 6600 Serial A027761790, JASCO Corporation, Japan), and Differential Scanning Colorimeter (DSC) (Model DSC200, XiangYi Instruments Co. Ltd, Xianglan City, China). The FTIR spectra was then compared with those of common polymers such as PP, HDPE, LDPE in OMNIC (9.11.727, Themo Fisher Scientific, MA, USA) (Proximate Analysis was done as per the ASTM standard (ASTM International, 2007) using A LabTech LDO – 150F electric oven Serial No.

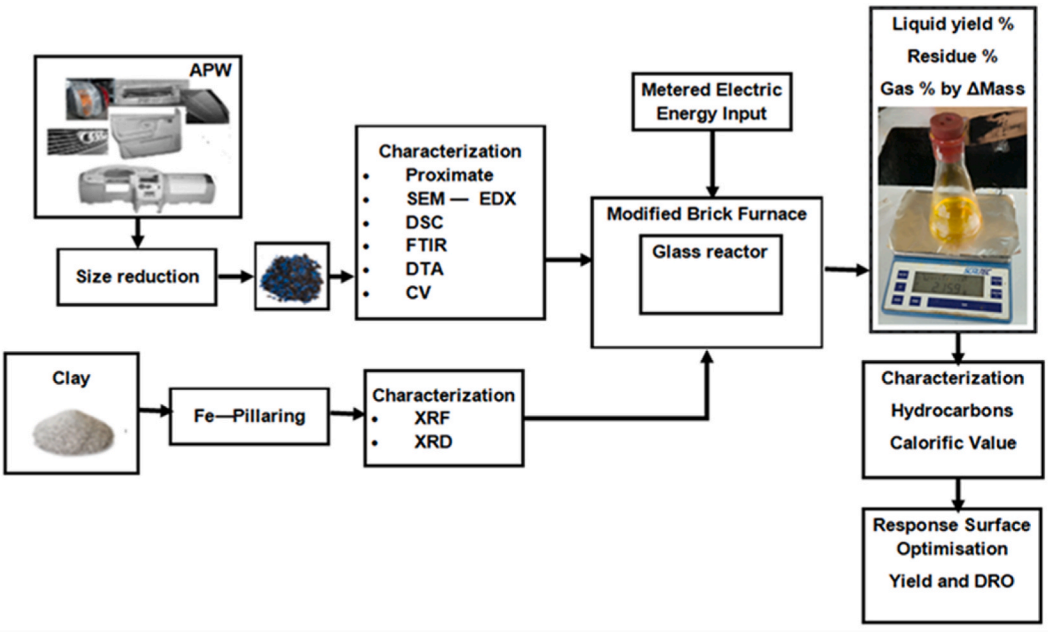

Fig. 1. Automotive plastic waste pyrolysis study methodology.

2018070203 (Daihan Labtech Co, Limited, Korea), and a Carbolite Gerbo ELF 11/14B electric furnace Serial No. 21–801916 (Carbolite Gero Ltd, United Kingdom). The morphology and carbon content determination were done using Scanning Electron Microscopy (SEM) with Energy Dispersive X-Ray Analysis (EDX), a Tescan VEGA 3 SBU Serial No. 118–0015 SEM (Tescan, Netherlands). Thermogravimetric analysis was done using a PerkinElmer Simultaneous Thermal Analyzer Model STA6000 Serial No. 521A17090106 (PerkinElmer, Inc., MA, USA).

2.2. Clay catalyst preparation and characterization

Bentonite clay samples were obtained from River Mining Co. in Kajiado, Kenya. The collected clay was oven dried, cooled and subsequently pulverized. The modification was done following the wet impregnation and pillaring technique described by Refs. [47,48]. To make the Fe pillaring solution, 0.1 mol l^{-1} $FeCl_3$ and NaOH solutions were prepared by dilution of $FeCl_3$ and NaOH pellets. The 0.1 mol l-1 $FeCl_3$ was then added dropwise to the 0.1 mol l^{-1} NaOH solution, keeping the pH at 2 and then the solution aged for 24 h under stirring every 20 min. The clay was pillared by wet impregnation. Here, a 0.5 g ml-1 clay suspension in water was mixed with the pillaring solution at a concentration of 2.5 mmol metal ion g^{-1} clay and stirred every 20 min for 24 h. The clay was then washed repeatedly with distilled water until the pH of filtrate became neutral, then sundried for 12 h and followed by 6 h at 105 °C. The clay was then heated to 150 °C at 20 °C.min^{-1} for 30 min and finally calcined at 300 °C for 1 h in an electric furnace to produce the iron pillared clay. The clay was sampled and analysed using X-ray Fluorescence Spectrophotometry (XRFS) analysis to determine the composition of the elements in oxide form e.g., Silica, Alumina. X-ray Diffraction (XRD) analysis was used to provide information on the crystallographic structure of the material.

2.3. Thermal and catalytic pyrolysis of automotive plastic waste to oil

Thermal and catalytic pyrolysis were carried out in a reactor that consisted of a 250 ml borosilicate round-bottomed flask, an electric – powered modified brick furnace, a 300 mm Liebig condenser and a weighing balance. Both thermal and catalytic pyrolysis was conducted. Measured responses included oil yield in grams, from which oil yield as a percentage of feedstock was calculated, mass of solid residue in grams from which the yield of residue as a percentage was determined. The yield of incondensable gas was determined by difference. The initial thermal pyrolysis runs included 350 °*C*, 400 °C, 428 °*C*, 450 °*C*, 500 °C, and was based on the decomposition temperatures observed from TGA and DSC studies. From observation of yield and consistency of the condensable fraction, a temperature range for the catalytic process, with a centre point at 400 °C. This was based on the combination of substantial yield of condensable fraction, and observed consistency of the oil produced around this temperature from the initial thermal runs.

A Central Composite Design with two factors at two levels was chosen. Thus, for the catalytic runs, temperature settings with a high of 420 °C and low of 380 °C, ensuring a mid-point temperature of 400 °C was used. This also resulted in axial point temperature settings of 428.3 °C and 371.7 °C which were subsequently rounded off to 428 °C and 372 °C respectively, due to the input threshold of the furnace temperature controller. Additional thermal runs were then added to ensure similar temperatures for both thermal and catalytic pyrolysis over the temperature range. Overall, the thermal pyrolysis process then consisted of nine runs conducted at 350 °C, 372 °C, 379 °C, 400 °C, 420 °C, 428 °C, 450 °C, 500 °C, and 521 °C.

The levels of clay catalyst amount used included a high of 30 % and low of 10 %. This wide range was chosen as most studies reported the best effect on oil yield in this range [29,36,44,49]. Axial point settings for clay amount were 34.14 and % 5.86 % wt. Catalytic pyrolysis runs ere therefore done over the temperature range 428 °C, 420 °C, 400 °C, 380 °C, and 372 °C, and clay catalyst amount 34.14 wt%, 30 wt%, 20 wt%, 10 wt%, and 5.86 % wt. These totalled 13 runs per set.

2.4. Characterization of chemical and physical properties of the oil yield

Gas Chromatography-Mass Spectrometry Analysis using a Shimadzu SE 2010-SE Serial No. 028534978858 (Shimadzu Corporation, Kyoto, Japan) was used to establish the hydrocarbon compounds present in the oil, and the NIST-14 library was used to match and identify the peaks. The area percentage of Diesel Range Organic C_8 – C_{24} and C_9 – C_{20} hydrocarbons was then calculated. According to Speight, and Gad [50,51], diesel is the fuel typically obtained over the boiling range of approximately 175 °C–375 °C, and have a carbon number range of C_8 - C_{24}, although C_9 – C_{20} hydrocarbons are predominant.

The calorific value (CV) of the liquid samples was determined using a Gallenkamp Bomb Calorimeter Model CAB001.AB1.C Serial No. SG96/02/536 (Gallenkamp Labs, Cambridge, United Kingdom). Kinematic Viscosity at 40 °C was determined as per ASTM D445 for determination of the kinematic viscosity of liquid petroleum products. The density at 20 °C was done as per ASTM D1298-12b (2017) Standard Test Method for Density, Relative Density, or API Gravity of Crude Petroleum and Liquid Petroleum Products by Hydrometer Method. The flash point was determined as per the ASTM D92-18 Standard Test Method for Flash and Fire Points by the Cleveland Open Cup Tester. The copper strip corrosion was determined as per ASTM D4048 – 19a Standard Test Method for Detection of Copper Corrosion from Lubricating Grease. These were then compared to the values reported in the ASTM D 975 Standard Specification for Diesel Fuel, EN 590:2009 - Automotive fuels – Diesel, and the specifications of categories 1 and 5 of the World Wide Fuel Charter.

2.5. Analysis and optimization of oil yield and diesel range hydrocarbon compounds

The CCD experimental design was used and analysed by Design Expert 13 and a suitable model was chosen with consideration of

the model F and p-values, correlation coefficient R^2, and whether or not aliasing was present in the model. The analysis of Variance was done at 95 % confidence interval. Three – dimensional response surfaces and contour plots were used to facilitate an examination of the influence of experimental variables on the responses. The maximum oil and DRO yields were determined using the optimization function in Design Expert 13. Additionally, for comparison between catalytic and thermal pyrolysis, responses obtained from similar temperature settings, that is;- 428 °C, 420 °C, 400 °C, 372 °C were compared by t – testing and examined using boxplots for similarity in yield.

3. Results and discussion

3.1. Composition of automotive plastic waste

The APW consisted mostly of front and back vehicle bumper which contributed 86.8 wt% of the sample. It contained a high volatile component (84.659 ± 4.099 wt%), high ash content (15.209 ± 3.977 wt%), and low fixed carbon (0.13 ± 0.046 w%). The high ash content was attributed to fibreglass used as fillers to strengthen the automotive components such as in Ref. [12] in which front bumper and interior accessories samples contained high (>18 %) ash also attributed to inorganic fillings, and Costa et al. [52], where bumper sample exhibited residual mass of 16.4 % above 900 °C, and further charateristion by inductively coupled plasma-optical emission spectroscopy (ICP-OES) revealed talc as the mineral filler. Glass fiber reinforcement or talc are the main mineral additives to automotive plastics [24].

The thermal decomposition was as shown in Fig. 2 where Fig. 2 (a), (b), (c) and (d) represent the dompisiton at heating rates of 5 K/min, 10 K/min, 15 K/min and 20 K/min respectively. The thermogravimetric study indicated that the decomposition rate was highest at 427 °*C* – 477 °*C*, and the sample achieved 95 % mass loss by 475 °*C*. This was similar to the range 375 °C–480 °C at which maximum rate of mass loss for various APW and tire samples occurred [12], and was in agreement with the decomposition temperatures of common plastic polymers such as PS, PP, LDPE, and HDPE, which was noted to vary from 350 °C to 500 °C, with maximum mass losses between 413 °C and 479 °C, similar to 480 °C for mixed Automotive Shredder Residue [53], and 450 °C–480 °C for mixed HDPE, LDPE, and PP in Kremer et al. [54], at 5–20 °C/min heating rates.

The activation energies were 216.3 kJ/mol, 216.7 kJ/mol, and 218.9 kJ/mol using the Kissinger, Flynn – Wall – Ozawa, and

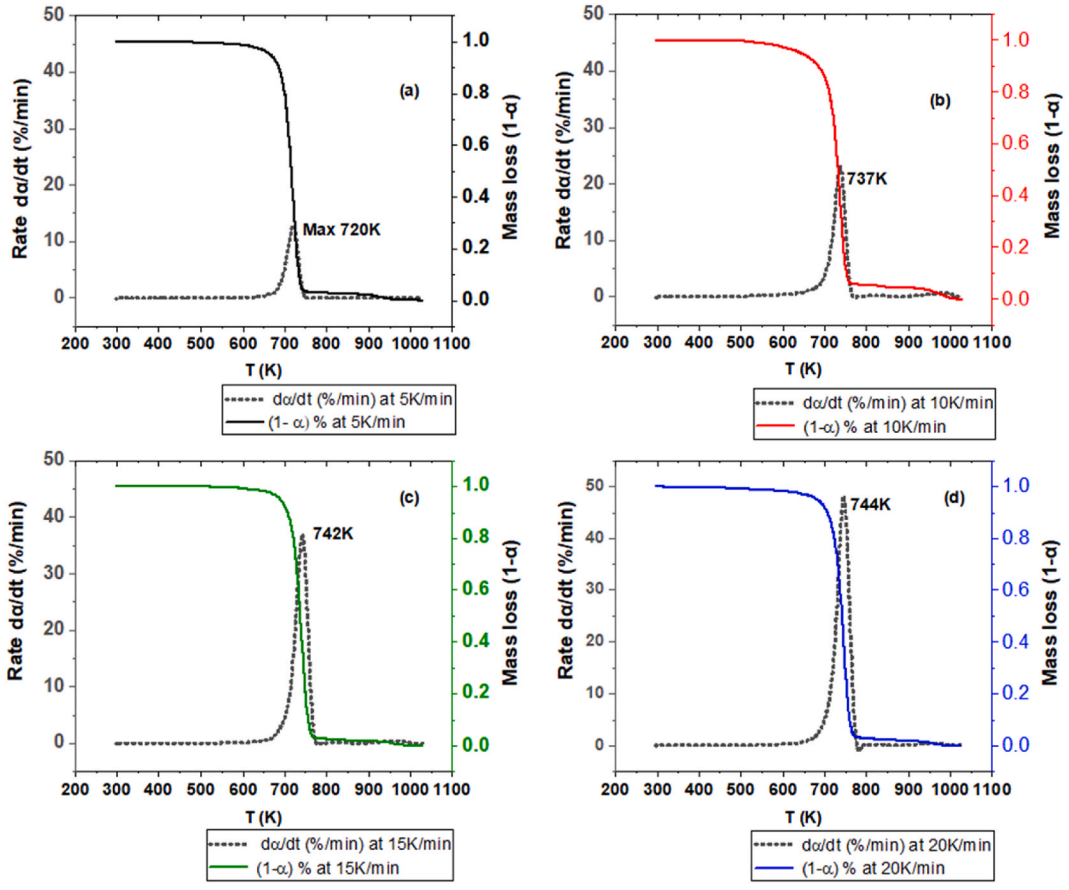

Fig. 2. Thermogravimetric analysis (TGA) mass loss curves at 5 (a), 10 (b), 15 (c), and 20K/min (d).

Freidman methods respectively [55]. These activation energies calculated using the several methods were within range of those of automotive plastic wastes, and mixed plastic wastes by other researchers such as; - 221 kJ/mol [56], 190–220 kJ/mol for PP [57], 231 kJ/mol for HDPE, 208 kJ/mol for LDPE, 193 kJ/mol for PP, 161 kJ/mol for PS, and 204 kJ/mol for mixed HDPE – LDPE – PP – PS [54]. They were however higher than 299.37 kJ/mol for HDPE, 227.46 kJ/mol for PP obtained by Ref. [58]. This could be a result of the use of virgin polymer samples by the researchers. Generally, waste polymers degrade more easily compared to virgin polymer samples, under thermal treatment [59]. As per the SEM analyses, the APW exhibited semi-crystalline (possibly indicating the presence of HDPE, LDPE, and PP) and amorphous polymer (possibly indicating the presence of ABS, PS and PC) characteristics [60]. The FTIR spectra for APW is shown in Fig. 3 (b) and its comparison with the spectra of virgin polymers as shown in Fig. 3(a).

Strong peaks at 2952, 2916 and 2848 cm^{-1} represent C-H stretching in methyl and methylene groups, indicating polypropylene, and polyethylene and polybutadiene [61,62]. A sharp peak at 2164 cm^{-1} corresponds to C ≡ N stretching, which suggested ABS presence [63]. Aromatic C-H stretching and bending are evident at 3000–3100 cm^{-1} and 1450–1495 cm^{-1}, respectively, confirming ABS and polystyrene (PS). Peaks at 1582 cm^{-1} and indicate C – C multiple-bond stretching in aromatic compounds [64] attributable to the aromatic rings in the ABS and PS chemical structures [65–67]. The medium peak at 1452 cm^{-1} corresponds to C – C multiple-bond stretching in aromatic compounds which occur as a medium peak at approximately 1500 cm^{-1}, and 1450 cm^{-1}. It also corresponds to the C – H bond bending in alkanes (CH_2 –) which occurs as a medium peak at 1485–1445 cm^{-1} [64] and is observed as a characteristic peak in the PP spectra. The 1374 cm^{-1} peak represents C-H bending in alkanes, characteristic of polypropylene. A peak at 1015 cm^{-1} suggests C-N vibrations, consistent with aliphatic compounds and ABS. Peaks at 876, 669, 535 and 405 cm^{-1} are attributed to C-H wagging, C-Cl stretching, C-X stretching and ring deformation in aromatic structures, respectively. These findings, along with spectral comparison, indicate a composite of predominantly polypropylene and high/low density polyethylene, with minor amounts of ABS, polystyrene, and fiberglass.

DSC analysis as shown in Fig. 4 identified endothermic peaks corresponding to the melting temperatures of ABS, HDPE, PP, and PS. These included a peak at approximately 138 °C corresponding to the melting temperature of ABS and HDPE [68,69]. A subsequent endothermic peak appeared at around 178 °C, corresponding to the melting temperature of PP [68] and lastly, an endothermic peak at approximately 231 °C was attributed to the melting temperature of PS [68,69].

The calorific value of the APW sample was determined as 37.76 MJ/kg, which was similar to those of automotive plastic components in Ref. [70] which averaged 36.119 ± 0.064 for various components including bumper, dashboard, reflector, pillar panel, wheel hub and others. It was however less than the calorific value typically observed for virgin and consumer plastics such as 46.3 MJ/kg (PE), 46.4 (PP) in Ref. [71] and 44.6 MJ/kg (PE, and PP) in Ielovich et al. [72].

3.2. Clay composition and silica – alumina ratio

The analysis of the clay using X – ray Fluorescence Spectrophotometry (XRFS) and X-ray Diffraction (XRD) to determine the composition, and crystallographic structure of the material. The XRFS result is as shown in Table 1. This showed that the Si/Al ratio of the pillared calcium bentonite clay catalyst was 3.06 ± 0.023, while that of unmodified calcium bentonite clay was 5.880. The clay comprised of silica polymorphs including cristobalite, tridymite and quartz. The Si/Al ratio has impact on the activity, selectivity, and stability zeolites [73]. A low Si/Al ratio is associated with higher surface acidity, and [43,74]. Thus, in this study, the modification increased surface acidity, and potentially improving catalytic activity.

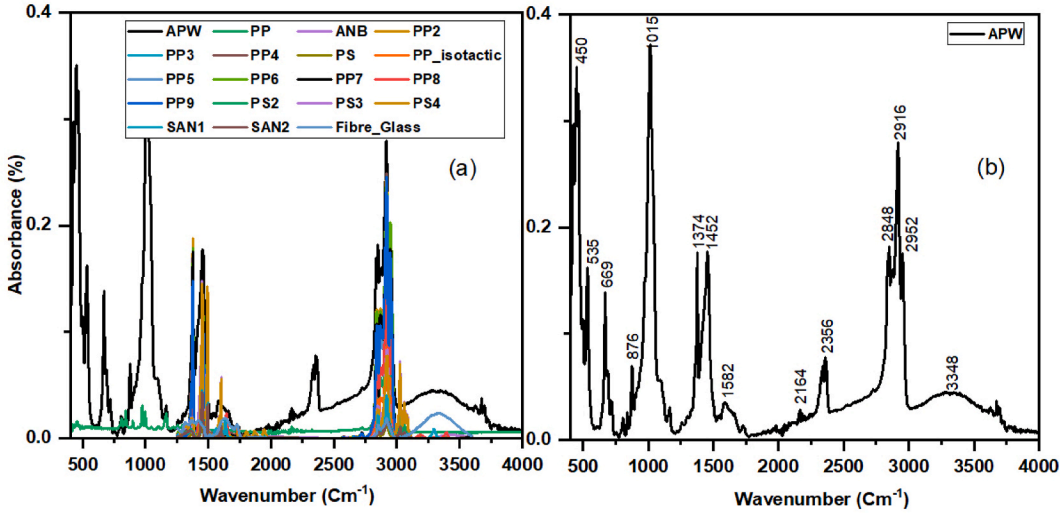

Fig. 3. FTIR spectra of APW sample (a), and comparison of FTIR spectra of APW sample with other polymer samples.

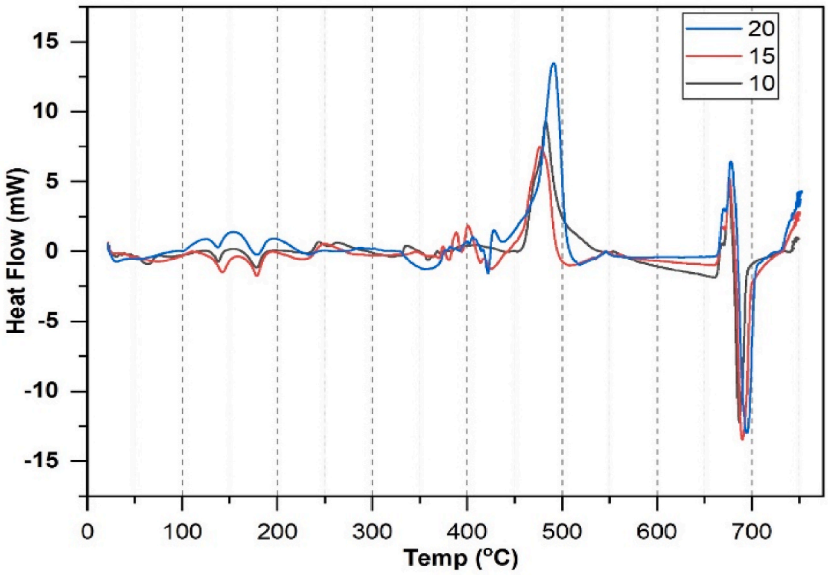

Fig. 4. DSC curves for the APW samples at 10, 15, and 20 K/min heating rate.

Table 1
Composition of Iron pillared calcium bentonite clay.

Mineral	Mass Percentage (%)	+/− (%)	Mineral	Mass Percentage (%)	+/− (%)
SiO2	55.535	0.81	Zr	0.026	0.001
Al2O3	18.011	0.734	Cu	0.025	0.003
CaO	8.399	0.07	Sn	0.016	0.025
Fe	8.347	0.078	V	0.014	0.006
S	3.02	0.072	Zn	0.014	0.002
MgO	2.833	2.65	P2O5	0.012	0.072
K2O	2.256	0.041	Rb	0.012	0.001
Ti	0.963	0.018	Y	0.005	0.001
Cl	0.269	0.029	Nb	0.005	0.001
Mn	0.088	0.013	Ni	0.003	0.003
Sr	0.074	0.002	As	0.001	0.001
Ba	0.072	0.031	Mo	0.001	0.002

3.3. Oil yield from thermal and catalytic pyrolysis of APW

3.3.1. Oil yield from thermal pyrolysis

Thermal pyrolysis of the APW samples between 350 °*C* to 521 °*C* yielded three products, condensable oil/wax, non-condensable gas, and solid residue. The yield of condensable oil/wax yield ranged from 15.9 % to 72.8 %. The oil, residue, and gas yields are as shown in Fig. 5.

Thermal pyrolysis oil yield generally increased with increase in temperature, with linear fitting resulting in Pearson's r of 0.84951, and an Adjusted R^2 of 0.6819. The residue yield reduced with increase in temperature, with liner fitting resulting in a Pearson's r of -0.91802, and an Adjusted R^2 of 0.82029. This pointed to increased thermal breakdown of the polymer structures with increase in temperature. This was expected as TGA results in Fig. 2 showed that degradation and conversion of APW increased with increase in temperature. The oil yield at 350 °C was lower than yield of 80.88 % for HDPE at 350 °C reported by Ahmad et al. [75], 40 % yield from bumper waste pyrolysis at 340 °C, and 32 % obtained during polyolefin film pyrolysis at 380 °C [13]. It as however comparable to the yield at 340 °C (40 %) reported by Kiran and Varuvel [76].

The oil produced below 450 °*C* was light and volatile, while that produced above 450 °*C* had a waxy consistency similar to petroleum jelly or lubricating grease. Similar observations were made by other researchers such as [77–80]. Panda [36], in his study using calcium Bentonite at various temperatures in the range 400–550 °C reported "*The pyrolysis of plastic samples yielded three different products: (i) the major product includes a volatile oil at lower temperature (400 and 450 °C) or a waxy oil at and above 475 °C*", while Singh [80] reported increase in wax above 550 °C. This tendency to produce waxy oil with increase in temperature is attributed to the reduced residence time of the vapour when the temperature was increased. This in turn was caused by the high pressure build up in the reactor due to the increased polymer decomposition and vapour production rate. The reduced residence time led to less cracking of the long-range hydrocarbon vapour produced from polymer feedstock decomposition, and thus the waxy product observed. Generally, the

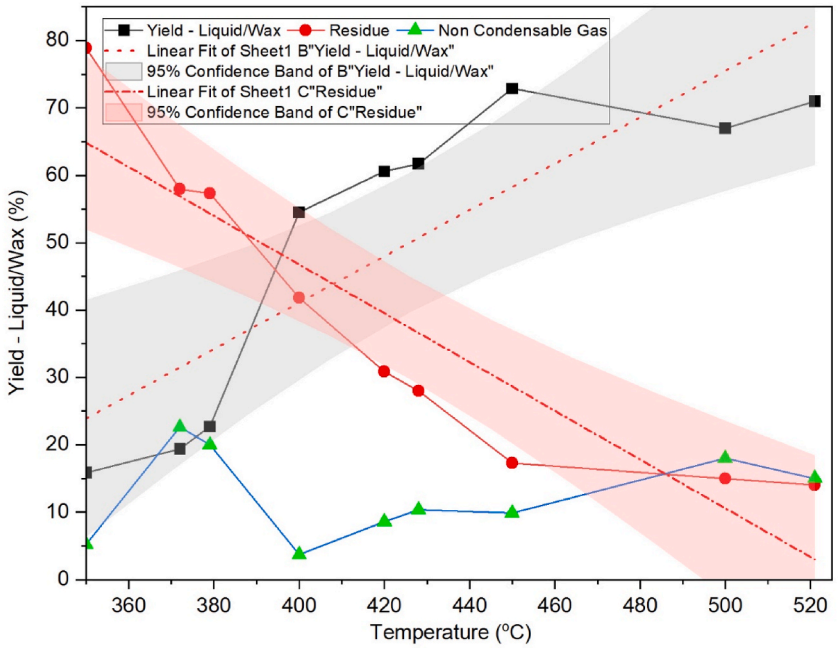

Fig. 5. Yield of condensable liquid/wax, residue, and non-condensable gas from thermal pyrolysis of APW.

yield was slightly less than those of waste consumer plastics used in other pyrolysis studies such as 70 % - 81 % (PP), and 69.8 %–80 % (HDPE) [81–83]. The results could be attributable to the fact that consumer polymers contain less additives such as fiberglass reinforcement, and thus have more volatile matter per unit mass which allows them to yield more volatile products upon thermal treatment. Expectedly, the oil yield was greater than that obtained from pyrolysis of automobile shredder residue such as in Refs. [84, 85]. This was likely due to the fact that ASR typically contains non-volatile components such as metals, as compared to only the plastic fraction of vehicle waste used in this study.

3.3.2. Oil yield from catalytic pyrolysis

The variation in oil yield with temperature and catalyst amount is shown in Fig. 5. The oil yield from catalytic pyrolysis varied from 47.86 % to 76.86 %, with an average of 68.12 % across the temperature range (371.7 $^{\circ}C$ – 428.3 $^{\circ}C$). Analysis of Variance testing of the oil yield response showed that a quadratic model was significant (F-value of 49.28, and p – value < 0.0001). While the five centre point showed variations in oil yield (73.284 $\pm$ 1.451 %) possibly attributable variations in plastic sample composition, and other errors, the lack of fit error was not significant relative to pure error (p – value = 0.1672). The quadratic model was thus used for further analysis of the effects of temperature and catalyst.

It was observed that an increase in temperature favoured higher oil/condensable yield, while the effect of the clay catalyst was

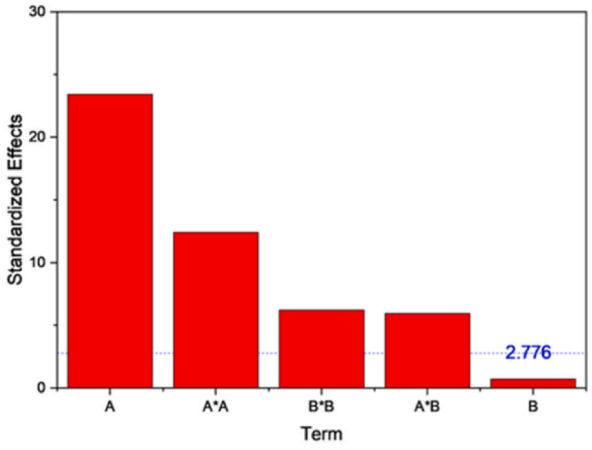

Fig. 6. Effect plot of temperature (A), catalyst (B), and the temperature - catalyst interaction (AB).

more nuanced. The maximum yield of catalytic pyrolysis in this study (76.86 %) was higher than in other studies containing PP, PS, H/LDPE and ABS. For example, the yield was higher than that reported by Ref. [86] for PP and HDPE pyrolysis, whereby the maximum yield was 68.77 % at 5 % clay – feedstock ratio for PP. It was also higher than 70.19 % for HDPE at 2.5 % clay – feedstock ratio using Acid Washed Bentonite Clay (AWBC) [86]. The maximum oil yield obtained was also higher 71.34 % 5 % clay – feedstock ratio for HDPE using iron-modified acid-washed bentonite Clay (Fe- AWBC) [48]. The maximum yield obtained was however less than 82.8 % at 1 % Clay – feedstock ration for PP, and who reported a yield of 79.3 % for pyrolysis of mixed plastic (42 % HDPE, 35 % PP, 18 % PS, 5 % PET) with Iron pillared bentonite [48].

i. Effect of temperature on oil yield

The effect of temperature on oil yield is shown in Fig. 6. Regression analysis showed that temperature had the largest effect of oil yield. However, the effect of temperature – catalyst interaction also led to the increase in oil yield. Analysis of variance showed that the quadratic model was significant. (Sequential p – value of 0.0006).

Temperature has the greatest effect (higher temperature led to higher oil yield). As can be observed in Fig. 7, the oil yield increased from 47.86 % to 76.86 % when temperature increased from 371.7 $^{\circ}C$ to 428.3 $^{\circ}C$. This is because as temperature was increased, the activation energy of the decomposition reaction decreased, and this allowed a larger fraction of the reactants to decompose, and at a higher rate. This led to a higher yield of both condensable and non-condensable volatiles. This was as seen in the thermogravimetric analysis where increase in temperature led to faster decomposition, and higher conversion, as such, this effect was expected. However, temperature as involved in temperature – catalyst interaction effects on oil yield, therefore the yield of oil at a given temperature was dependent on the amount of clay catalyst.

ii. Effect of clay on oil yield

The bentonite clay exhibited a bifunctional effect as observed in Fig. 8. Low amounts of clay (−1, that is 10 %) reported low oil yield. The yield then increased peaking at around the midpoint (0, 20 %). Further increase in clay amount led to reduced oil yield. The improved oil yield in clay catalysis was attributable to the its high surface acidity as shown by the relatively low Silica – Alumina (Si/Al) ratio of 3.06 ± 0.023 which meant the presence of sufficient aluminium that provided acid sites due to its valence and presence of mesopores [29,33,40,41,87]. This allowed the clay to act as a Brønsted acid [88], and facilitated the mechanism of the reaction by the formation of the hydride ion or the addition of a proton [74,89,90] thus leading to relatively more cracking and secondary reactions. The reduction in oil yield with further increase of catalyst amount above 20 % could probably due to heat transfer limitations in the batch reactor used, and not the effect of the catalyst intrinsically. The yield of oil could be expected to increase if clay catalyst was used in a reactor with more uniform heat transfer such as a fluidized bed reactor compared to the reactor used in this study.

iii. Interaction effects. While oil yield was highly dependent on temperature as shown in Fig. 8(a), rather than clay amount as shown in Fig. 8(b), interaction effects of temperature and catalyst amount was significant. This can be seen in the two-way interaction plot shown in Fig. 8(c). Low temperature led to low oil yield at both low and high clay amounts, underscoring the substantial temperature dependence of the process. At higher temperature, the yield is generally higher, but the effect of clay catalyst is more observable. However, at higher temperature, moderate to high clay amount (20 %–30 %) led to improvement in oil yield. This can be seen in Fig. 8 (c), where temperature – catalyst interaction effect led to higher oil yield at higher temperature. At low clay amount and low temperature, the interaction effect leads to substantial reduction in yield of oil. Thus, from the main and interaction effect plots, it was predictable that to maximize oil yield, a high temperature, and moderate to high amount of clay catalyst was required.

3.3.3. Comparison of thermal and catalytic pyrolysis oil yield

The oil yield for catalytic pyrolysis was generally higher than that of thermal pyrolysis. Over the common temperature range

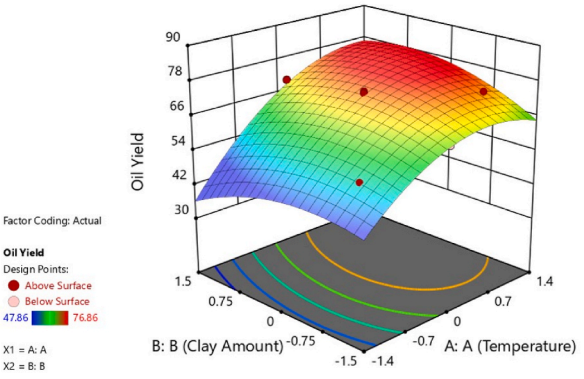

Fig. 7. Surface plot of oil yield from catalytic pyrolysis.

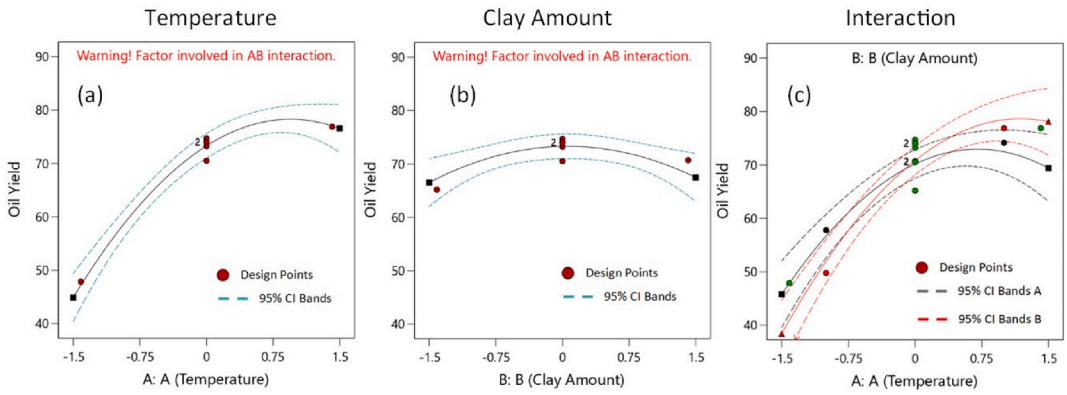

Fig. 8. Effect of temperature (a) and clay amount (b), and interaction effects (c).

372 °C–428 °C, the oil yield for thermal pyrolysis was 40.63 ± 18.50 %, while the catalytic pyrolysis yield over the same temperature range was 68.12 ± 9.61 %. This comparison is shown in Fig. 9. The box plot shows that catalytic pyrolysis had a higher mean and median oil yield, with less variation, while thermal pyrolysis reported a lower mean and median yields, and wider variation in yield between the runs. This difference in oil yield was confirmed by paired t – testing of the yields at 5 % confidence level. The test showed that yield for catalytic pyrolysis was significantly higher (p – value = 0.0097) than that of thermal pyrolysis, and thus confirmed that the modified clay catalyst increased oil yield.

3.4. Diesel range organics yield from thermal and catalytic pyrolysis of APW

3.4.1. Composition of commercial diesel fuel

Analysis of the diesel fuel sample showed that it comprised mostly of C_8 – C_{24} hydrocarbons (95.36 area%), with most of the compounds in the range C_9 – C_{20} (67.75 %), representing mostly the paraffinic/saturated hydrocarbons. This was in agreement with the composition of petroleum diesel established by Ref. [91]. The most abundant hydrocarbons in the diesel sample were C_{11} – C_{20}, compounds, the majority of these were paraffinic hydrocarbons, which included 10-Methyleicosane (peaks 12–17, 27.61 area%), Pentadecane (peaks 9 and 11, 20.21 %), and Dodecane (peaks 6 and 7, 15.03 area%). Other abundant compounds were Tetradecane (peak 8, 11.32 area%), Undecane (peaks 4 and 5, 10.18 area%), and Hexadecane (peak 10, 9.72 area%). These compounds made up 94 area% of the diesel fuel. The chromatograph for the diesel fuel sample was as shown in Fig. 10. The identified peaks for thermal pyrolysis oil at 372 °C and catalytic pyrolysis oil at 372 °C and 20 % catalyst are shown in Table 2, Table 3, Table 4 respectively.

3.4.2. FTIR analysis of catalytic pyrolysis oil

Pyrolysis oil samples produced at the highest temperature and lowest temperature of during catalytic pyrolysis, that is; - 428 °C, and 372 °C, and both at 20 % catalyst amount were analysed by FTIR and compared to a diesel fuel sample. This was as shown in the spectra in Fig. 11. By observation of the plot, the similarities in the broad outlook were apparent between the diesel and pyrolysis oil samples. This was observed by the occurrence of the - CH_3 (methyl) asymmetrical stretch strong peak in aliphatic hydrocarbons

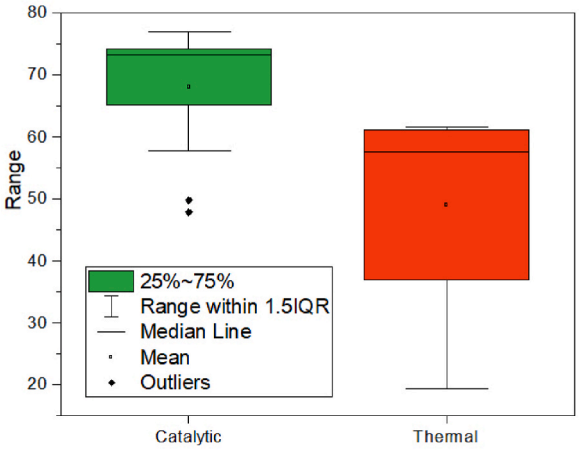

Fig. 9. Box Plot of the oil yield from thermal, and catalytic pyrolysis processes.

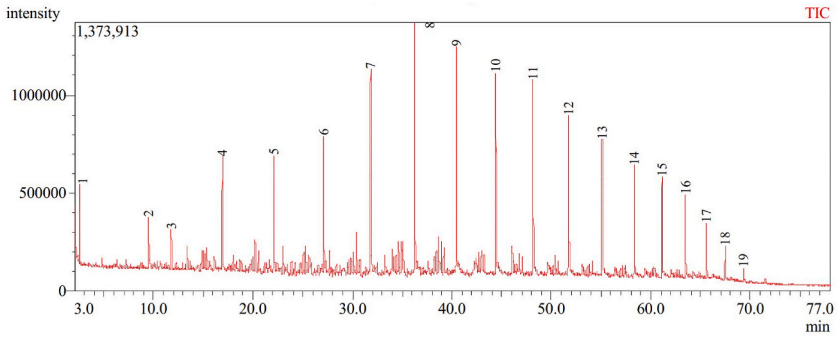

Fig. 10. Chromatograph of commercial diesel fuel sample.

Table 2
Commercial diesel sample chromatograph peaks.

Peak#	R.Time	Area	Area%	Height	Height%	Name
1	2.599	598528	1.50	399433	3.56	n-Hexane
2	9.512	653521	1.64	239359	2.14	2-Pentanone, 4-hydroxy-4-methyl-
3	11.791	513603	1.29	173560	1.55	Nonane
4	16.930	2093546	5.24	558977	4.99	Undecane
5	22.099	1971047	4.94	567443	5.06	Undecane
6	27.098	2498830	6.26	681214	6.08	Dodecane
7	31.810	3502319	8.77	984455	8.78	Dodecane
8	36.259	4520493	11.32	1240842	11.07	Tetradecane
9	40.448	4200076	10.52	1115320	9.95	Pentadecane
10	44.409	3881368	9.72	997868	8.90	Hexadecane
11	48.152	3868420	9.69	950270	8.48	Pentadecane
12	51.723	2785503	6.98	731300	6.53	Eicosane, 10-methyl-
13	55.111	2538291	6.36	671023	5.99	Eicosane, 10-methyl-
14	58.338	2069466	5.18	540937	4.83	Eicosane, 10-methyl-
15	61.131	1630389	4.08	483974	4.32	Eicosane, 10-methyl-
16	63.493	1221215	3.06	401935	3.59	Eicosane, 10-methyl-
17	65.573	780526	1.95	261897	2.34	Eicosane, 10-methyl-
18	67.461	399025	1.00	146093	1.30	2-methyloctacosane
19	69.305	207339	0.52	61275	0.55	Tetracosane, 11-decyl-
		39933505	100.00	11207175	100.00	

(2952.4 cm^{-1}, 2954.4 cm^{-1}, and 2955.4 cm^{-1} for diesel, pyrolysis oil at 428 °C/20 % catalyst, and pyrolysis oil at 372 °C/20 % catalyst respectively), CH_2 asymmetric stretch strong peak (2920.7 cm^{-1}, 2921.6 cm^{-1}, and 2921.6 cm^{-1} for diesel, pyrolysis oil at 428 °C/20 % catalyst, and pyrolysis oil at 372 °C/20 % catalyst respectively), as well as the CH_3 symmetric strong stretch (2852.2 cm^{-1}, 2853.2 cm^{-1}, and 2870.5 cm^{-1} for diesel, and pyrolysis oil at 428 °C/20 % catalyst, and pyrolysis oil at 372 °C/20 % catalyst respectively). These show presence of alkane hydrocarbon compounds [64]. The existence of diesel range organics was also confirmed by the medium peaks indicative of C – H bending bond of the methylene group in alkanes and C – C olefin bonds. These peaks occur at 1460.8 cm^{-1} in the commercial diesel sample, 1456.99 cm^{-1} in the pyrolysis oil at 372 °C/20 % catalyst, and at 1456.96 cm^{-1} in the pyrolysis oil produced at 428 °C/20 %.

3.4.3. DRO yield from thermal pyrolysis

The oil from thermal pyrolysis contained $C_6 – C_{10}$ (52.31 ± 3.50 area%), C_9 - C_{20} (73.91 ± 4.08 area%), C_8 - C_{24} (82.92 ± 4.39 area %) and C_{25}+ (6.48 ± 1.99 area %) as shown in Fig. 12 (a). The C_8 - C_{24} hydrocarbons which was less than the fraction present in the diesel sample (95.36 %). In addition, oil from thermal pyrolysis contained significantly more $C_6 – C_{10}$ (52.31 ± 3.50 area %) than diesel fuel (4.43 area%), and it also contained more C_{25}+ (6.48 ± 1.99 area %) than diesel fuel (1.52 area%). The C_8 - C_{24} yield generally reduced with increase in temperature (Pearson's r = 0.79198, and Adjusted R^2 = 0.57398 for linear fit). Over the same temperature range, The $C_6 – C_{10}$ yield generally increased as indicated by Pearson's r = 0.84572, and Adjusted R^2 = 0. 67455. This could be due to increased cracking of Diesel Range to Gasoline Range Organics with increase in temperature. (see Fig. 13)

The most abundant hydrocarbons across all thermal runs were unsaturated hydrocarbons (41.81 ± 7.94 %) as shown in Fig. 12 (b). , and this was greater than typically found in diesel fuel. The most abundant compound was 2,4-Dimethyl-1-heptene (25.37 ± 2.01 %), similar to that for PP thermal pyrolysis (2,4-Dimethyl-1-heptene, 15.08 %) obtained by Ref. [92], and to the oil product from car bumper pyrolysis in Ref. [70] which comprised of a similarly high amount of 2,4-Dimethylhept-1-ene (35.65 area%). It was also noted as a major constituent of PP thermal pyrolysis in Ref. [93]. This high yield of unsaturated organics was attributable to the backbiting reactions after C – C bond scission.

Table 3
Pyrolysis oil (produced at 372 °C and 20 % catalyst amount) chromatograph peaks.

Peak#	R.Time	Area	Area%	Height	Height%	Name
1	2.342	474468	1.01	294540	1.90	Pentane, 2-methyl-
2	2.522	1368023	2.92	862954	5.56	1-Pentene, 2-methyl-
3	2.598	1255298	2.68	873589	5.63	n-Hexane
4	2.686	285191	0.61	200338	1.29	2-Pentene, 2-methyl-
5	3.184	367766	0.78	178726	1.15	1-Pentene, 2,4-dimethyl-
6	6.029	713207	1.52	300654	1.94	Pentane, 2,3,4-trimethyl-
7	8.559	697614	1.49	251236	1.62	2-Hexene, 4,4,5-trimethyl-
8	8.684	342957	0.73	119179	0.77	Cyclohexane, 1,3,5-trimethyl-
9	8.969	9758438	20.83	3424277	22.07	2,4-Dimethyl-1-heptene
10	9.509	870478	1.86	287709	1.85	2-Pentanone, 4-hydroxy-4-methyl-
11	9.774	504998	1.08	172621	1.11	Cyclohexane, 1,3,5-trimethyl-, (1.alpha.,3.al
12	11.330	1234010	2.63	423788	2.73	2-Pentanone, 3-[(acetyloxy)methyl]-3,4-dime
13	11.784	850998	1.82	226951	1.46	Styrene
14	16.411	172866	0.37	59699	0.38	3-Methyl-2-butenoic acid, 3-phenylpropyl es
15	16.526	187528	0.40	65293	0.42	Cyclopropane, 1-heptyl-2-methyl-
16	17.191	574829	1.23	179673	1.16	Decane, 4-methyl-
17	17.419	528064	1.13	167060	1.08	Decane, 4-methyl-
18	20.778	1813987	3.87	518695	3.34	1-Dodecanol, 3,7,11-trimethyl-
19	21.000	1286557	2.75	368797	2.38	2-Undecene, 4,5-dimethyl-, [R*,S*-(Z)]-
20	21.711	304056	0.65	90058	0.58	1-Dodecene
21	23.159	292150	0.62	95618	0.62	1-Decene, 2,4-dimethyl-
22	24.397	448601	0.96	131301	0.85	(2,4,6-Trimethylcyclohexyl) methanol
23	26.733	225817	0.48	68113	0.44	3-Tetradecene, (Z)-
24	27.089	179412	0.38	53858	0.35	Dodecane
25	30.200	219868	0.47	73059	0.47	2-Decene, 2,4-dimethyl-
26	31.671	4021310	8.58	1106503	7.13	11-Methyldodecanol
27	32.063	1482032	3.16	357683	2.31	11-Methyldodecanol
28	32.440	3303470	7.05	899545	5.80	1-Undecene, 7-methyl-
29	33.596	574088	1.23	164249	1.06	2-Hexyl-1-octanol
30	34.810	485892	1.04	141330	0.91	Cyclododecanemethano
31	35.953	189961	0.41	65128	0.42	3-Tetradecene, (Z)-
32	36.240	178586	0.38	59154	0.38	Tetradecane
33	40.862	1062370	2.27	298971	1.93	Octadecyl trifluoroacetate
34	41.978	650728	1.39	156306	1.01	Pentadecafluorooctanoic acid, tetradecyl este
35	43.674	556160	1.19	165753	1.07	(2,4,6-Trimethylcyclohexyl) methanol
36	48.882	1583967	3.38	407344	2.63	Tricosyl trifluoroacetate
37	49.945	1365526	2.91	250730	1.62	1-Dodecanol, 2-hexyl-
38	51.074	500471	1.07	145328	0.94	Tricosyl trifluoroacetate
39	51.443	533684	1.14	155397	1.00	2-Propylhept-3-enoic acid, phenylthio ester
40	56.059	824652	1.76	217551	1.40	Tetracosyl trifluoroacetate
41	58.398	644718	1.38	198090	1.28	Cyclooctane, 1-methyl-3-propyl-
42	62.051	749428	1.60	237034	1.53	Tetracosyl trifluoroacetate
43	62.640	402288	0.86	129190	0.83	Octacosyl trifluoroacetate
44	63.749	1008420	2.15	320189	2.06	Cyclohexane, 1,2,3,5-tetraisopropyl-
45	66.456	531263	1.13	164876	1.06	Hexatriacontyl trifluoroacetate
46	67.840	701866	1.50	253708	1.64	Cyclohexane, 1,2,3,5-tetraisopropyl-
47	72.236	545376	1.16	133167	0.86	Cyclohexane, 1,2,3,5-tetraisopropyl-
		46853437	100.00	15515012	100.00	

3.4.4. DRO yield from catalytic pyrolysis

The oil from catalytic pyrolysis contained $C_6 - C_{10}$ (43.07 ± 8.07 area%), $C_9 - C_{20}$ (73.67 ± 4.05 area%), $C_8 - C_{24}$ (81.81 ± 3.60 area%) and $C_{25}+$ (6.62 ± 1.85 area%). The $C_8 - C_{24}$ DRO yield was lower than that from commercial diesel. The oil contained 42.53 ± 7.75 % unsaturated hydrocarbons, 9.59 ± 2.87 % cyclic hydrocarbons, 4.67 ± 2.96 area% aromatic hydrocarbons. The most abundant hydrocarbon was 2, 4 – Dimethyl – 1 – heptane (23.44 ± 2.42 area%). Additionally, the oil contained 18.91 ± 6.03 area% alcohols, and 2.41 ± 1.51 area%% organic acids as shown in Fig. 11. Yield of saturated, unsaturated, cyclic, aromatic, alcohol, and organic acid compounds.

The yield of diesel range organics was similar to that of catalytic pyrolysis of PP using bentonite clay catalysts (86.18 area%%) obtained in Ref. [92]. It was however different from the yield of 99.95 % $C_8 - C_{24}$ and 0.05 % $C_{25}+$ for pyrolysis of HDPE with Ni – W – ZSM – 5 catalysts at 360 °*C* in Ref. [94]. This implied that Ni – W – ZSM – 5 exhibited better catalytic effect in influencing product distribution, compared to calcium bentonite clay. The large presence of $C_6 - C_{10}$ GRO indicated over cracking of the liquid produced due to high temperature, and high surface acidity [43], which enhanced secondary reactions. Oil Fuel Properties.

3.4.5. Comparison of thermal and catalytic pyrolysis DRO yield

The $C_8 - C_{24}$ DRO yield for thermal pyrolysis was generally higher than that of catalytic pyrolysis as seen in Fig. 12. Over the common temperature range 372 °C–428 °C, $C_8 - C_{24}$ DRO yield for thermal pyrolysis was 83.22 ± 4.07 area%, while the catalytic

Table 4
Pyrolysis oil (produced at 372 °C, thermal) chromatograph peaks.

Peak#	R.Time	Area	Area%	Height	Height%	Name
1	2.341	984176	1.23	701559	2.75	Pentane, 2-methyl-
2	2.521	2451911	3.06	1700745	6.66	1-Pentene, 2-methyl-
3	3.181	806102	1.00	447800	1.75	1-Pentene, 2,4-dimethyl-
4	6.030	1845323	2.30	774297	3.03	Hexane, 2,3-dimethyl-
5	6.313	392303	0.49	135553	0.53	Toluene
6	7.734	383397	0.48	127108	0.50	Cyclopentane, 1,1,3,4-tetramethyl-, cis-
7	8.078	551513	0.69	202511	0.79	Heptane, 2,4-dimethyl-
8	8.688	722792	0.90	247978	0.97	Cyclohexane, 1,3,5-trimethyl-
9	8.974	17664110	22.01	6143889	24.04	2,4-Dimethyl-1-heptene
10	9.516	738987	0.92	244876	0.96	2-Pentanone, 4-hydroxy-4-methyl-
11	9.778	984374	1.23	328216	1.28	Cyclohexane, 1,3,5-trimethyl-, (1.alpha.,3.alpha.,5.beta.)
12	10.482	579295	0.72	154916	0.61	1,2,4,4-Tetramethylcyclopentene
13	10.866	597989	0.75	191850	0.75	1,2,4,4-Tetramethylcyclopentene
14	11.335	4243394	5.29	1379956	5.40	2-Pentanone, 3-[(acetyloxy)methyl]-3,4-dimethyl-, (.+-.)
15	11.783	1992498	2.48	514515	2.01	Styrene
16	16.409	678656	0.85	172886	0.68	Bicyclo[4.2.0]octa-1,3,5-triene, 3-methyl-
17	17.201	1573763	1.96	460923	1.80	Decane, 4-methyl-
18	17.424	1530545	1.91	455378	1.78	Decane, 4-methyl-
19	20.785	4050085	5.05	1132222	4.43	1-Dodecanol, 3,7,11-trimethyl-
20	21.007	3429217	4.27	970779	3.80	2-Undecene, 4,5-dimethyl-, [R*,S*-(Z)]-
21	23.166	968457	1.21	278632	1.09	1-Decene, 2,4-dimethyl-
22	23.491	781265	0.97	213554	0.84	1-Decene, 2,4-dimethyl-
23	24.406	690353	0.86	205331	0.80	(2,4,6-Trimethylcyclohexyl) methano
24	28.448	232064	0.29	82340	0.32	Dodecane, 4,6-dimethyl-
25	28.859	388721	0.48	113005	0.44	Dodecane, 4,6-dimethyl-
26	29.175	457808	0.57	128312	0.50	Dodecane, 2,6,11-trimethyl-
27	31.683	7153983	8.92	2027789	7.93	11-Methyldodecanol
28	32.076	3798135	4.73	920353	3.60	11-Methyldodecanol
29	32.454	6144534	7.66	1687091	6.60	1-Undecene, 7-methyl-
30	33.603	1828578	2.28	496911	1.94	2-Hexyl-1-octanol
31	34.597	1452149	1.81	403471	1.58	2-Hexyl-1-octano
32	34.820	798848	1.00	225758	0.88	Cyclododecanemethanol
33	38.396	369139	0.46	109155	0.43	Dodecane, 2,6,11-trimethyl-
34	40.878	1841014	2.29	475628	1.86	1-Dodecanol, 2-hexyl-
35	41.279	1153357	1.44	242667	0.95	Pentadecafluorooctanoic acid, tetradecyl ester
36	41.988	1355186	1.69	304604	1.19	Octadecyl trifluoroacetate
37	42.380	543527	0.68	149553	0.59	Pentadecafluorooctanoic acid, tetradecyl ester
38	42.525	283176	0.35	95728	0.37	1-Dodecanol, 2-hexyl-
39	43.686	565939	0.71	163348	0.64	(2,4,6-Trimethylcyclohexyl) methanol
40	48.900	1313758	1.64	348568	1.36	Tricosyl trifluoroacetate
41	49.965	1414511	1.76	260426	1.02	Octacosyl trifluoroacetate
42	51.085	504467	0.63	135304	0.53	1-Dodecanol, 2-hexyl-
		80239399	100.00	25555485	100.00	

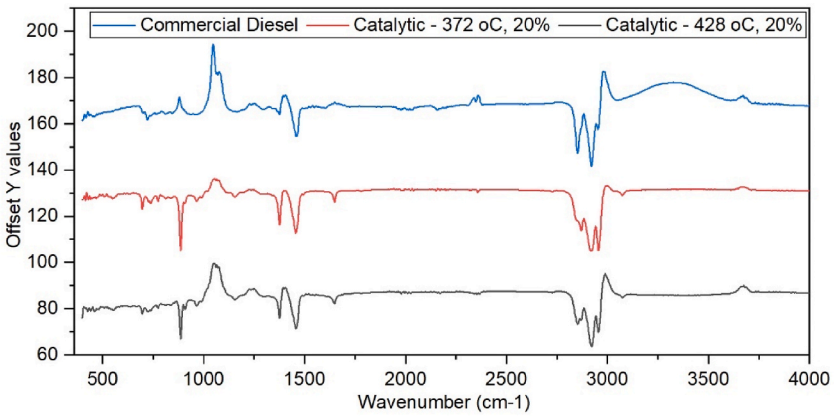

Fig. 11. FTIR spectra of oil produced by at 428 °C, 20 % and 372 °C and 20 %.

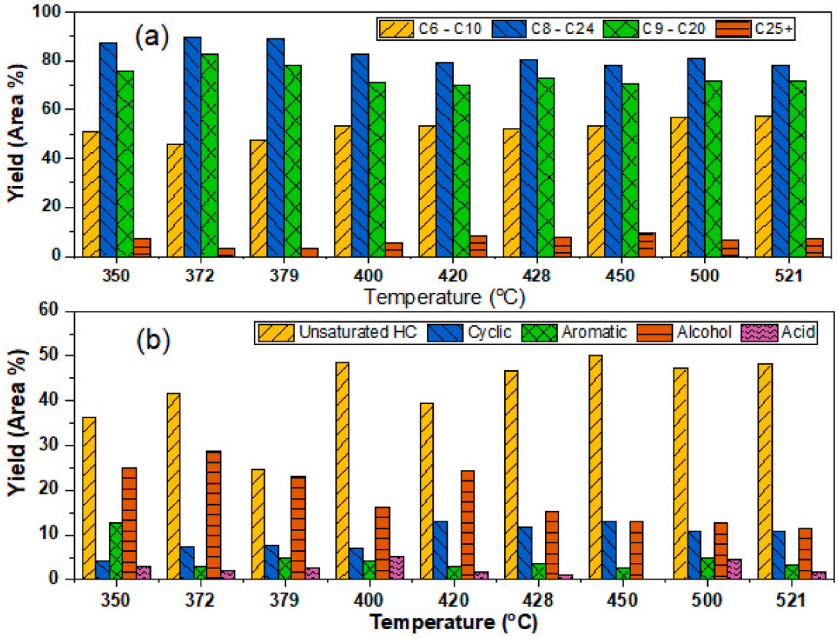

Fig. 12. Yield of C_6 – C_{10}, C_9 – C_{20}, C_8 – C_{24}, and C_{25}+ and unsaturated, cyclic, aromatic, alcohol, and organic acid compounds from thermal pyrolysis of APW.

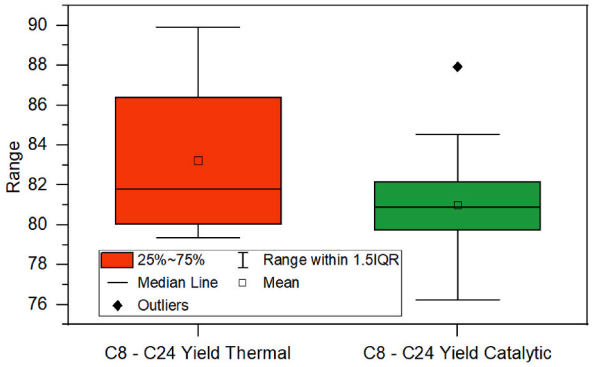

Fig. 13. Box Plot of the C8 - C24 DRO yield from thermal, and catalytic pyrolysis processes.

pyrolysis yield over the same temperature range was 81.00 ± 3.15 area%. This comparison is shown in Fig. 9. The box plot shows that thermal pyrolysis had a higher mean and median C_8 – C_{24} DRO yield than catalytic. Paired t – testing of the yields at 5 % confidence level showed that this difference was not significant (p – value = 0.4270), and thus confirmed that the modified clay catalyst did not increase DRO yield.

3.4.6. Reaction mechanisms and effect of catalyst

Catalysts can influence the kinetics, and the mechanisms of the reaction, thereby influencing the product distribution, and thus, the abundance of paraffins and olefins, and comparatively small amount of cyclic (10.05 ± 1.72 area%), and aromatic compounds (3.55 ± 1.21 area%) implied that the formation of majority of products could be explained by carbonium ion mechanisms [95] for both PP and H/LDPE.

Catalytic decomposition of L/HDPE involved initial protolysis of the polymer (C_nH_{2n+2}) with Brønsted acid sites (H^+S^-) to yield paraffinic hydrocarbons and the surface carbonium ions. This was then followed by the propagation reaction, which involves disproportionation between the surface carbonium ions formed, and the feed molecules to yield paraffins. This was then followed by β-scission of the surface carbonium ion to form olefin products, leaving smaller carbonium ions on the catalyst surface. Sufficiently small olefins may desorb from catalyst surfaces, while others surface olefins may be protonated to form new carbonium ions. The reactions are then terminated by destruction of surface carbonium ions such as by desorption to produce olefins and regenerate Brønsted acid sites.

The product distribution in this study was similar to those reported by PP pyrolysis in Refs. [96,97], and bumper pyrolysis in Ref. [12] which showed enhanced C_8 to C_{10} production. This indicated that catalytic decomposition of PP involved degradation of polymer to oligomer to liquid, then to gas [97,98]. The most important of the elementary reactions being the so called back – biting reactions in which intramolecular rearrangements take place via a six-membered transition state to inner tertiary carbon atoms, forming the C_9 fraction [99]. The backbiting reactions in this mechanism explained the high abundance of the trimer (2,4-dimethyl-1-heptene), n-pentane, 2-methyl-1- pentene (dimer) in plastics pyrolysis as in in Perez and Toraman [99] and explained by Kruse [100]. It could also explain the observed abundance of 2,4-Dimethyl-1-heptene, and 2-methyl-1-Pentene which was the most abundant and third most abundant hydrocarbons obtained in this study. The mechanism also explained the abundance to 2-methyl-1--Pentene which is the dimer formed from C – C bond cleave from the trimer, and provided insights into product formations for both catalytic and thermal pyrolysis.

3.5. Pyrolysis oil fuel properties

The properties of the catalytic pyrolysis oil obtained are shown in Table 5**.** These are presented alongside the recommended values as per the ASTM D975: Standard Specification for Diesel Fuel Oils, EN 590:2009 Automotive fuels - Diesel - Requirements and test methods, and the 6th Edition of the World-Wide Fuel Charter: Gasoline and diesel published by the International Organization of Motor Vehicle Manufacturers. For the World-Wide Fuel Charter, two sets of values are provided, Category 1 for markets with no or first-level requirements for emission control, and category 5 for markets with highly advanced requirements for emission control. The flash point of the APW catalytic pyrolysis oil obtained was within the recommended range, thus the fuel can be stored and transported safely using conventional means.

The density and kinematic viscosity of the oil obtained was higher than recommended in the standards, except for the kinematic viscosity of No. 4 diesel oil specified in the ASTM D975 for which it was within range. This likely resulted from the high amount of C_{25}+ hydrocarbons which averaged 6.18 ± 2.02 %, compared to that of commercial diesel fuel tested (1.52 %). High temperature (and low residence time) with low catalyst amount promoted higher yield of this fraction thus the requirement for lower temperature, or higher residence time to produce less dense and viscous oil. Alternatively other methods can be applied to reduce this heavy fraction, including simple distillation, or centrifugation. According to the [101], higher density favours higher particulate emissions in all diesel vehicles, and also higher NOx emissions in heavy-duty vehicles, although it increases power output, and reduces fuel consumption. As such, the density and kinematic viscosity of the APW pyrolysis oil only reduces a slight reduction to enhance suitability as automotive diesel fuel.

The fraction of aromatic hydrocarbons in the pyrolysis oil was within the recommended for diesel fuels. Low quantity of aromatics is required because a higher content of aromatics increases the flame temperature during combustion and thus resulted in increased NOx emissions, and in addition, low aromatic content favours reduced particulates emissions [101].

4. Conclusions

The following three main conclusions were drawn from this study: Firstly, APW is suitable for recycling by pyrolysis based on the findings from its characterization. Its properties such as high volatiles content, high carbon content, decomposition temperatures, and activation energies were similar to those of consumer plastics such as HDPE, LDPE, PP, and PS which have been shown by other researchers to be recyclable into fuels product. Secondly, APW pyrolysis produces a relatively high yield of oil which is necessary for viability of its recycling into oil products. As shown by ANOVA, using the modified clay (Fe – PILC) significantly increased the yield of oil obtained from APW pyrolysis compared to thermal pyrolysis. Thirdly, APW pyrolysis yields oil with organic composition similar to commercial diesel. It contained substantial amounts of $C_8 – C_{24}$ and $C_9 – C_{20}$ organic compounds. As the results showed, this was true for both thermal and catalytic pyrolysis. The study also showed that showed that using the modified clay did not significant affect the yield of $C_8 – C_{24}$ and $C_9 – C_{20}$ as indicated by regression and subsequent ANOVA. Lastly, to obtain both high yield of oil and high yield of $C_8 – C_{24}$ a high temperature and moderate clay amount were required, and the physicochemical such as flash point, calorific value, and fraction of aromatic compounds were similar to those of diesel fuel, while others such as density, kinematic viscosity, and copper strip corrosion were outside the range specified in common diesel fuel standards. Thus, pyrolysis is therefore suitable method of recycling APW to oil products, and the yield of oil can be enhanced by the use of iron pillared bentonite clay. The clay however does not significantly affect the yield of diesel range organic compounds in the oil produced. The oil produced has some similarity to diesel fuel, although it requires further processing.

Table 5
Catalytic pyrolysis oil fuel properties.

Property	Test Method	Test Result	ASTM D 975	EN 590:2009	WWFC Category 1	WWFC Category 5
Calorific Value (MJ/kg)	ASTM D240-19	49.85	N/A	N/A	N/A	N/A
Flash point (°C)	ASTM D 92	113.2	≥38	≥55	≥55	≥55
Viscosity at 40 °C (mm^2/S)	ASTM D 445	10.4	≤24.0 (No. 4 D)	≤4.5	≤4.5	≤4.0
Density (kg/m^3)	ASTM D 1298	1.102		≤845 (at 15o)	≤860 (at 15)	≤840 (at 15)
Copper strip corrosion	ASTM D 4048	2e	3	1	1	1
	Total Aromatics	3.55 ± 1.21 Area %	≤35 % v/v	≤11 % m/m	≤15 % m/m	≤15 % m/m

Since this study was limited to thermal pyrolysis and the use of iron pillared catalyst at a fixed concentration of Iron (III) ion, further investigation of catalytic pyrolysis of APW using modified clay prepared with varying concentration of the Iron (III) ion should be conducted. This would be able to show whether different concentrations of iron in the catalyst would still increase the oil yield, and more importantly, increase the yield of diesel range organics, and a comparison between clay, modified clay, and commercial catalysts can be considered. As this study showed that the yield of gasoline range organic compounds was relatively abundant, a strategy of maximizing pyrolysis oil product with both gasoline range and diesel range organics, followed by a separation process to make two products – diesel and gasoline should be investigated as an alternative to optimizing for diesel range organics only. This could potentially eliminate the need to use a catalyst. Pyrolysis coupled with GC (py – GC) should be used to study the pyrolysis process. This would generate more data points that would be useful in analyzing yield of DRO, and to aid modelling and simulation of possible plant scale operation. Such modelling and simulation, when combined with economic analysis would establish the technical and economic feasibility of commercial and plant scale operation.

The vehicle scrapping policy and mechanisms for management of end-of-life vehicles as recommended in Kenya's national automotive policy of 2022 should be developed in other developing countries, with establishment of standards for after sales service, maintenance and repair developed to include stripping and segregation of plastic components from end-of-life vehicles by the service provider to be accredited and licensed. This will enable collection of data on automotive plastic waste generation which are generally limited. This will support planning for the development of commercial and economically feasible industrial scale recycling operations.

CRediT authorship contribution statement

Elly Olomo: Writing – review & editing, Writing – original draft, Software, Methodology, Investigation, Funding acquisition, Formal analysis, Data curation, Conceptualization. **Stephen Talai:** Writing – review & editing, Validation, Supervision, Resources, Project administration, Methodology, Investigation, Formal analysis, Data curation, Conceptualization. **Joseph Kiplagat:** Writing – review & editing, Validation, Supervision, Methodology, Investigation, Formal analysis, Conceptualization. **Egide Manirambona:** Writing – review & editing, Visualization, Investigation. **Anthony Muliwa:** Writing – original draft, Visualization, Validation, Supervision, Methodology, Formal analysis, Data curation, Conceptualization. **Jasper Okino:** Writing – original draft, Validation, Methodology, Investigation, Conceptualization.

Data availability

Data will be made available on request.

Declaration of competing interest

The authors declare that they have no known competing financial interests or personal relationships that could have appeared to influence the work reported in this paper.

Acknowledgements

This research was funded by the Mobility for Innovative Renewable Energy Technologies (MIRET) project, under Intra-Africa Academic Mobility Scheme of the European Union at Moi University.

References

[1] UNEP, "Beat Plastic Pollution." [Online]. Available: https://www.unep.org/interactive/beat-plastic-pollution/.
[2] UNEP, Monitoring plastics in rivers and lakes: guidelines for the harmonization of methodologies, Nairobi - Kenya (2020).
[3] UNEP, "Used vehicles and the invironment: a global overview of used light duty vehicles: flow, Scale and Regulation (2020).
[4] American Chemistry Council, "Transitioning toward a circular economy for automotive plastics and, Polym. Compos. (2020), https://doi.org/10.18356/5d9e0035-en.
[5] S. Aditya Pradeep, R.K. Iyer, H. Kazan, S. Pilla, Automotive applications of plastics: past, present, and future, in: Applied Plastics Engineering Handbook: Processing, Materials, and Applications, second ed., Elsevier Inc., Oxford, 2017 https://doi.org/10.1016/B978-0-323-39040-8.00031-6.
[6] H. Abedsoltan, Applications of plastics in the automotive industry: current trends and future perspectives, Polym. Eng. Sci. 64 (3) (2024) 929–950, https://doi.org/10.1002/pen.26604.
[7] G. Guo, K. Fan, Z. Guo, W. Guo, Pyrolysis behavior of automotive polypropylene plastics: ReaxFF molecular dynamics study on the co-pyrolysis of polypropylene and EPDM/POE, Energy 280 (2023) 128202, https://doi.org/10.1016/j.energy.2023.128202.
[8] Ellen MacArthur Foundation, The new plastics economy: rethinking the future of plastics & catalysing action. https://doi.org/10.1103/Physrevb.74.035409, 2017.
[9] Ellen MacArthur Foundation, "The Global Commitment 2020 Progress Report," (2020).
[10] Jyoti Agarwal, S. Sahoo, S. Mohanty, S.K. Nayak, Progress of novel techniques for lightweight automobile applications through innovative eco-friendly composite materials: a review, J. Thermoplast. Compos. Mater. 33 (7) (2020) 978–1013, https://doi.org/10.1177/0892705718815530.
[11] EuRIC, EuRIC Call for Recycled Plastic Content in Cars, Position Paper, 2020.
[12] I. Čabalová, A. Ház, J. Krilek, T. Bubeníková, J. Melicherčík, T. Kuvik, Recycling of wastes plastics and tires from automotive industry, Polymers 13 (13) (Jul. 2021) 2210, https://doi.org/10.3390/polym13132210.
[13] N. Netsch, et al., Chemical recycling of polyolefinic waste to light olefins by catalytic pyrolysis, Chem. Ing. Tech. 95 (8) (Aug. 2023) 1305–1313, https://doi.org/10.1002/cite.202300078.
[14] M. Chandran, S. Tamilkolundu, C. Murugesan, Conversion of Plastic Waste to Fuel. Plastic Waste and Recycling, Elsevier Inc., 2020, https://doi.org/10.1016/b978-0-12-817880-5.00014-1.

[15] S. Han, Y.-C. Jang, Y.-S. Choi, S.-K. Choi, Thermogravimetric kinetic study of automobile shredder residue (ASR) pyrolysis, Energies 13 (6) (2020), https://doi.org/10.3390/en13061451.
[16] Y. Ren, et al., Feasibility study on Co-processing of automobile shredder residue in coal-fired power plants via pyrolysis, Waste Manag. 143 (2022) 135–143, https://doi.org/10.1016/J.WASMAN.2022.02.028.
[17] C. Löwer and I. Verpraet, "Playing catch-up in plastics recycling for automotive production," Automot. Manuf. Solut. Accessed: Jul. 12, 2021. [Online]. Available: https://www.automotivemanufacturingsolutions.com/composites/playing-catch-up-in-plastics-recycling-for-automotive-production/41618.article.
[18] G. Musongwa, EgideManirambona, S.M. Talai, A.M. Muliwa, Combustion and emission characteristics of distilled waste plastic pyrolysis oil-gasoline blends using single cylinder motorcycle petrol engine, Int. J. Sustain. Eng. 17 (1) (2024) 46–55, https://doi.org/10.1080/19397038.2024.2358908.
[19] C. Stallkamp, M. Hennig, R. Volk, D. Stapf, F. Schultmann, Pyrolysis of mixed engineering plastics: economic challenges for automotive plastic waste, Waste Manag. 176 (March) (2024) 105–116, https://doi.org/10.1016/j.wasman.2024.01.035.
[20] P. Pilát, M. Patsch, Utilization of the energy potential of waste from the automotive industry, MATEC Web of Conferences 369 (Nov. 2022) 03004, https://doi.org/10.1051/matecconf/202236903004.
[21] T. Maqsood, J. Dai, Y. Zhang, M. Guang, B. Li, Pyrolysis of plastic species: a review of resources and products, J. Anal. Appl. Pyrolysis 159 (2021) 105295, https://doi.org/10.1016/j.jaap.2021.105295.
[22] Y. Cui, Y. Zhang, L. Cui, Y. Liu, B. Li, W. Liu, Microwave-assisted pyrolysis of polypropylene plastic for liquid oil production, J. Clean. Prod. 411 (2023) 137303, https://doi.org/10.1016/j.jclepro.2023.137303.
[23] S. Valizadeh, et al., Recent advances in liquid fuel production from plastic waste via pyrolysis: emphasis on polyolefins and polystyrene, Environ. Res. 246 (2024) 118154, https://doi.org/10.1016/j.envres.2024.118154.
[24] C. Stallkamp, M. Hennig, R. Volk, D. Stapf, F. Schultmann, Pyrolysis of mixed engineering plastics: economic challenges for automotive plastic waste, Waste Manag. 176 (Mar. 2024) 105–116, https://doi.org/10.1016/j.wasman.2024.01.035.
[25] H.M. Valladares Montemayor, R.H. Chanda, Automotive industry's circularity applications and industry 4.0, Environmental Challenges 12 (Aug. 2023) 100725, https://doi.org/10.1016/j.envc.2023.100725.
[26] A.L. Brooks, S. Wang, J.R. Jambeck, The Chinese Import Ban and Its Impact on Global Plastic Waste Trade (2018).
[27] J. Huang, A. Veksha, W.P. Chan, A. Giannis, G. Lisak, Chemical recycling of plastic waste for sustainable material management: a prospective review on catalysts and processes, Renew. Sustain. Energy Rev. 154 (Feb. 2022) 111866, https://doi.org/10.1016/j.rser.2021.111866.
[28] L. Dai, et al., Recent advances in polyolefinic plastic pyrolysis to produce fuels and chemicals, J. Anal. Appl. Pyrolysis 180 (2024) 106551, https://doi.org/10.1016/j.jaap.2024.106551.
[29] K. Li, et al., Fe-, Ti-, Zr- and Al-pillared clays for efficient catalytic pyrolysis of mixed plastics, Chem. Eng. J. 317 (2017) 800–809, https://doi.org/10.1016/j.cej.2017.02.113.
[30] M. Chandran, S. Tamilkolundu, C. Murugesan, Conversion of plastic waste to fuel, in: Plastic Waste and Recycling, Elsevier Inc., 2020, pp. 385–399, https://doi.org/10.1016/b978-0-12-817880-5.00014-1.
[31] S.H. Gebre, M.G. Sendeku, M. Bahri, Recent trends in the pyrolysis of non-degradable waste plastics, ChemistryOpen 10 (12) (2021) 1202–1226, https://doi.org/10.1002/open.202100184.
[32] R. Miandad, et al., Catalytic pyrolysis of plastic waste: moving toward pyrolysis based biorefineries, Front. Energy Res. 7 (MAR) (Mar. 2019), https://doi.org/10.3389/fenrg.2019.00027.
[33] G. Fadillah, I. Fatimah, I. Sahroni, M.M. Musawwa, T.M.I. Mahlia, O. Muraza, Recent progress in low-cost catalysts for pyrolysis of plastic waste to fuels, Catalysts 11 (7) (2021), https://doi.org/10.3390/catal11070837.
[34] E. Borsella, R. Aguado, A. De Stefanis, M. Olazar, Comparison of catalytic performance of an iron-alumina pillared montmorillonite and HZSM-5 zeolite on a spouted bed reactor, J. Anal. Appl. Pyrolysis 130 (2018) 249–255, https://doi.org/10.1016/j.jaap.2017.12.015.
[35] A. De Stefanis, P. Cafarelli, F. Gallese, E. Borsella, A. Nana, G. Perez, Catalytic pyrolysis of polyethylene: a comparison between pillared and restructured clays, J. Anal. Appl. Pyrolysis 104 (2013) 479–484, https://doi.org/10.1016/j.jaap.2013.05.023.
[36] A.K. Panda, Thermo-catalytic degradation of different plastics to drop in liquid fuel using calcium bentonite catalyst, Int. J. Integrated Care 9 (2) (2018) 167–176, https://doi.org/10.1007/s40090-018-0147-2.
[37] I.G. Hakeem, F. Aberuagba, U. Musa, Catalytic pyrolysis of waste polypropylene using Ahoko kaolin from Nigeria, Appl Petrochem Res 8 (4) (2018) 203–210, https://doi.org/10.1007/s13203-018-0207-8.
[38] L.O. Mark, M.C. Cendejas, I. Hermans, The use of heterogeneous catalysis in the chemical valorization of plastic waste, ChemSusChem 13 (22) (Nov. 2020) 5808–5836, https://doi.org/10.1002/cssc.202001905.
[39] A. Gil, M.A. Vicente, Progress and perspectives on pillared clays applied in energetic and environmental remediation processes, Curr. Opin. Green Sustainable Chem. 21 (2020) 56–63, https://doi.org/10.1016/j.cogsc.2019.12.004.
[40] A.C.S. Serra, J. V Milato, J.G. Faillace, M.R.C.M. Calderari, Reviewing the use of zeolites and clay based catalysts for pyrolysis of plastics and oil fractions, Braz. J. Chem. Eng. (2022), https://doi.org/10.1007/s43153-022-00254-2.
[41] J.G. Faillace, C.F. de Melo, S.P.L. de Souza, M.R. da Costa Marques, Production of light hydrocarbons from pyrolysis of heavy gas oil and high density polyethylene using pillared clays as catalysts, J. Anal. Appl. Pyrolysis 126 (2017) 70–76, https://doi.org/10.1016/j.jaap.2017.06.023.
[42] J. Lei, et al., Investigation on thermal dechlorination and catalytic pyrolysis in a continuous process for liquid fuel recovery from mixed plastic wastes, J. Mater. Cycles Waste Manag. 20 (1) (2018) 137–146, https://doi.org/10.1007/s10163-016-0555-3.
[43] G. Fadillah, I. Fatimah, I. Sahroni, M.M. Musawwa, T.M.I. Mahlia, Oki Muraza, Recent progress in low-cost catalysts for pyrolysis of plastic waste to fuels, Catalysts 11 (7) (2021), https://doi.org/10.3390/catal11070837.
[44] UNEP, Used vehicles and the environment: a global overview of used light duty vehicles: flow. Scale and Regulation, 2020.
[45] M.S.C. Stallkamp, "Designing a Circular Economy for Plastics: The Role of Chemical Recycling in Germany," (2023).
[46] D. Stapf, Chemical recycling of plastics waste – a contribution to a climate-neutral circular carbon economy, Chem. Ing. Tech. 94 (9) (Sep. 2022), https://doi.org/10.1002/cite.202255205.
[47] J.G. Faillace, C.F. de Melo, S.P.L. de Souza, M.R. da C. Marques, Production of light hydrocarbons from pyrolysis of heavy gas oil and high density polyethylene using pillared clays as catalysts, J. Anal. Appl. Pyrolysis 126 (2017) 70–76, https://doi.org/10.1016/j.jaap.2017.06.023.
[48] K. Li, et al., Fe-, Ti-, Zr- and Al-pillared clays for efficient catalytic pyrolysis of mixed plastics, Chem. Eng. J. 317 (2017) 800–809, https://doi.org/10.1016/j.cej.2017.02.113.
[49] Z.M. Chepchirchir, CATALYTIC PYROLYSIS OF PLASTIC WASTE TO LIQUID FUEL USING, Moi University, 2021.
[50] S.C. Gad, Diesel fuel, in: Encyclopedia of Toxicology, third ed., vol. 2, Elsevier, 2014, pp. 115–118, https://doi.org/10.1016/B978-0-12-386454-3.00837-X.
[51] J.G. Speight, Handbook of industrial hydrocarbon processes [Online]. Available: https://www.sciencedirect.com/book/9780128099230/handbook-of-industrial-hydrocarbon-processes, 2019.
[52] C.S. Costa, M. Muñoz, M.R. Ribeiro, J.M. Silva, A thermogravimetric study of HDPE conversion under a reductive atmosphere, Catal. Today (2020), https://doi.org/10.1016/j.cattod.2020.07.021.
[53] S. Han, Y.C. Jang, Y.S. Choi, S.K. Choi, Thermogravimetric kinetic study of automobile shredder residue (ASR) pyrolysis, Energies 13 (6) (2020), https://doi.org/10.3390/en13061451.
[54] I. Kremer, T. Tomić, Z. Katančić, Z. Hrnjak-Murgić, M. Erceg, D.R. Schneider, Catalytic decomposition and kinetic study of mixed plastic waste, Clean Technol. Environ. Policy 23 (3) (2021) 811–827, https://doi.org/10.1007/s10098-020-01930-y.
[55] M.J. Starink, The determination of activation energy from linear heating rate experiments : a comparison of the accuracy of isoconversion methods, Thermochim. Acta 404 (2003) 163–176, https://doi.org/10.1016/S0040-6031(03)00144-8.
[56] N. Miskolczi, T. Juzsakova, J. Sója, Preparation and application of metal loaded ZSM-5 and y-zeolite catalysts for thermo-catalytic pyrolysis of real end of life vehicle plastics waste, J. Energy Inst. 92 (1) (2019) 118–127, https://doi.org/10.1016/j.joei.2017.10.017.

[57] S.R. Chandrasekaran, B. Kunwar, B.R. Moser, N. Rajagopalan, B.K. Sharma, Catalytic thermal cracking of postconsumer waste plastics to fuels. 1. Kinetics and optimization, Energy Fuel. 29 (9) (2015) 6068–6077, https://doi.org/10.1021/acs.energyfuels.5b01083.
[58] J. Briceno, M.A. Lemos, F. Lemos, Kinetic analysis of the degradation of HDPE+PP polymer mixtures, Int. J. Chem. Kinet. 53 (5) (2021) 660–674, https://doi.org/10.1002/kin.21472.
[59] K. Pielichowski, J. Njuguna, T.M. Majka, Thermal Degradation of Polymeric Materials, second ed., Elsevier, Inc, 2023.
[60] M. Kutz, Applied Plastics Engineering Handbook, second ed., William Andrew (Elsevier, Oxford, 2017 https://doi.org/10.1016/c2014-0-04118-4.
[61] S.K. Vijayan, M.A. Kibria, M.H. Uddin, S. Bhattacharya, Pretreatment of automotive shredder residues, their chemical characterisation, and pyrolysis kinetics, Sustainability 13 (19) (2021), https://doi.org/10.3390/su131910549.
[62] B. Yang, M. Chen, Py–FTIR–GC/MS analysis of volatile products of automobile shredder residue pyrolysis, Polymers 12 (11) (2020) 2734, https://doi.org/10.3390/polym12112734.
[63] R. Khanna, M. Ikram-ul-haq, A. Rawal, R. Rajarao, Formation of carbyne-like materials during low temperature pyrolysis of lignocellulosic biomass : a natural resource of linear sp carbons, Sci. Rep. (August) (2017) 1–8, https://doi.org/10.1038/s41598-017-17240-1.
[64] L.G. Wade, J.W. Simek, Organic Chemistry, Pearson Education, 2016.
[65] M.R. Jung, et al., Validation of ATR FT-IR to identify polymers of plastic marine debris , including those ingested by marine organisms, Mar. Pollut. Bull. 127 (2018) 704–716, https://doi.org/10.1016/j.marpolbul.2017.12.061.
[66] S. Primpke, M. Wirth, C. Lorenz, G. Gerdts, Reference Database Design for the Automated Analysis of Microplastic Samples Based on Fourier Transform Infrared (FTIR) Spectroscopy, 2018, pp. 5131–5141.
[67] A.R. Shahmoradi, N. Talebibahmanbigloo, A.A. Javidparvar, G. Bahlakeh, B. Ramezanzadeh, Studying the adsorption/inhibition impact of the cellulose and lignin compounds extracted from agricultural waste on the mild steel corrosion in HCl solution, J. Mol. Liq. 304 (2020) 112751, https://doi.org/10.1016/j.molliq.2020.112751.
[68] J.P. Greene, Microstructures of polymers, Automotive Plastics and Composites (Jan. 2021) 27–37, https://doi.org/10.1016/B978-0-12-818008-2.00009-X.
[69] M. Rahman, N.R. Schott, L.K. Sadhu, Glass Transition of ABS in 3D Printing, Comsol, Boston, 2016, p. 3.
[70] Cabalová, et al., Recycling of wastes plastics and tires from automotive industry, Polymers 13 (2210) (2021).
[71] K. Handawy, A.Y.S. M, V. V Stepanov, V.A. Talalov, Energy recovery strategies as a sustainable solutions for municipal solid waste in Egypt, IOP Conf. Ser. Mater. Sci. Eng. 1100 (1) (2021) 012052, https://doi.org/10.1088/1757-899X/1100/1/012052.
[72] M. Ioelovich, Energy potential of natural, synthetic polymers and waste materials - a review, Academic Journal of Polymer Science 1 (1) (2018).
[73] K.E. Marak, L. Nandy, D. Jain, M.A. Freedman, Significance of the surface silica/alumina ratio and surface termination on the immersion freezing of ZSM-5 zeolites, Chem. Phys. 25 (16) (2023) 11442–11451, https://doi.org/10.1039/D2CP05466C.
[74] S.J. Park, et al., Catalytic pyrolysis of HDPE over WOx/Al2O3: effect of tungsten content on the acidity and catalytic performance, Mol. Catal. 528 (August) (2022) 112439, https://doi.org/10.1016/J.MCAT.2022.112439.
[75] I. Ahmad, et al., Pyrolysis study of polypropylene and polyethylene into premium oil products, Int. J. Green Energy 12 (7) (Jul. 2015) 663–671, https://doi.org/10.1080/15435075.2014.880146.
[76] S. Kiran, E.G. Varuvel, Pyrolytic conversion of automotive bumper polywaste to diesel like fuel and its utilization in compression ignition engine, Fuel 318 (Jun. 2022) 123559, https://doi.org/10.1016/j.fuel.2022.123559.
[77] D.G. Kulas, A. Zolghadr, D.R. Shonnard, Liquid-fed waste plastic pyrolysis pilot plant: effect of reactor volume on product yields, J. Anal. Appl. Pyrolysis 166 (2022) 105601, https://doi.org/10.1016/j.jaap.2022.105601.
[78] A.K. Panda, Thermo-catalytic degradation of different plastics to drop in liquid fuel using calcium bentonite catalyst, Int. J. Integrated Care 9 (2) (2018) 167–176, https://doi.org/10.1007/s40090-018-0147-2.
[79] R.K. Singh, B. Ruj, A.K. Sadhukhan, P. Gupta, Impact of fast and slow pyrolysis on the degradation of mixed plastic waste: product yield analysis and their characterization, J. Energy Inst. 92 (6) (2019) 1647–1657, https://doi.org/10.1016/j.joei.2019.01.009.
[80] R.K. Singh, B. Ruj, Time and temperature depended fuel gas generation from pyrolysis of real world municipal plastic waste, Fuel 174 (2016) 164–171, https://doi.org/10.1016/j.fuel.2016.01.049.
[81] I. Ahmad, et al., Influence of metal-oxide-supported bentonites on the pyrolysis behavior of polypropylene and high-density polyethylene, J. Appl. Polym. Sci. 132 (1) (2014) 1–19, https://doi.org/10.1002/app.41221.
[82] F. Sembiring, C.W. Purnomo, S. Purwono, Catalytic pyrolysis of waste plastic mixture, IOP Conf. Ser. Mater. Sci. Eng. (1) (2018) 316, https://doi.org/10.1088/1757-899X/316/1/012020.
[83] S.M.R. Mirkarimi, S. Bensaid, D. Chiaramonti, Conversion of mixed waste plastic into fuel for diesel engines through pyrolysis process: a review, Appl. Energy 327 (December) (2022), https://doi.org/10.1016/j.apenergy.2022.120040.
[84] N. Miskolczi, Z. Czégény, Thermo-catalytic pyrolysis of waste plastics from end of life vehicle, in: MATEC Web of Conferences 02, 2016.
[85] M. Zeller, N. Netsch, F. Richter, H. Leibold, D. Stapf, Chemical recycling of mixed plastic wastes by pyrolysis – pilot scale investigations, Chem. Ing. Tech. 93 (11) (2021) 1763–1770, https://doi.org/10.1002/cite.202100102.
[86] I. Ahmad, et al., Pyrolysis study of polypropylene and polyethylene into premium oil products, Int. J. Green Energy 12 (7) (2014) 663–671, https://doi.org/10.1080/15435075.2014.880146.
[87] X. Li, et al., Sustainable catalytic strategies for the transformation of plastic wastes into valued products, Chem. Eng. Sci. 276 (Jul. 2023) 118729, https://doi.org/10.1016/j.ces.2023.118729.
[88] F.M.T. Luna, J.A. Cecilia, R.M.A.B. Saboya, D.K. Sapag, E. Rodríguez-Castellón, C.L. Cavalcante, Natural and modified montmorillonite clays as catalysts for synthesis of biolubricants, Materials 11 (9) (2018) 6–9, https://doi.org/10.3390/ma11091764.
[89] A. De Stefanis, P. Cafarelli, F. Gallese, E. Borsella, A. Nana, G. Perez, Catalytic pyrolysis of polyethylene: a comparison between pillared and restructured clays, J. Anal. Appl. Pyrolysis 104 (2013) 479–484, https://doi.org/10.1016/j.jaap.2013.05.023.
[90] I.G. Hakeem, F. Aberuagba, U. Musa, Catalytic pyrolysis of waste polypropylene using ahoko kaolin from Nigeria, Appl Petrochem Res 8 (4) (2018) 203–210, https://doi.org/10.1007/s13203-018-0207-8.
[91] J.G. Speight, Handbook of Industrial Hydrocarbon Processes (2019).
[92] S. Budsaereechai, A.J. Hunt, Y. Ngernyen, Catalytic pyrolysis of plastic waste for the production of liquid fuels for engines, RSC Adv. 9 (10) (2019) 5844–5857, https://doi.org/10.1039/c8ra10058f.
[93] T.M. Kruse, H.W. Wong, L.J. Broadbelt, Mechanistic modeling of polymer pyrolysis: polypropylene, Macromolecules 36 (25) (2003) 9594–9607, https://doi.org/10.1021/ma030322y.
[94] M. Arnold, B. Boghosian, M. Li, Catalytic production of diesel-like oils from plastic wastes, J. Renew. Sustain. Energy 13 (6) (2021) 064701, https://doi.org/10.1063/5.0066218.
[95] W. Kaminsky, J. Scheirs, Feedstock Recycling and Pyrolysis of Waste Plastics: Converting Waste Plastics into Diesel and Other Fuels, John Wiley & Sons, Ltd, 2006.
[96] K. Murata, Effect of porous solid in catalytic degradation of polymers, SCIREA Journal of Energy 7 (1) (2022) 1–16, https://doi.org/10.54647/energy48156.
[97] Y. Ishihara, H. Nanbu, K. Saido, T. Ikemura, T. Takesue, T. Kuroki, Mechanism of gas formation in catalytic decomposition of polypropylene, Fuel 72 (8) (Aug. 1993) 1115–1119, https://doi.org/10.1016/0016-2361(93)90318-V.
[98] R.E. Harmon, G. SriBala, L.J. Broadbelt, A.K. Burnham, Insight into polyethylene and polypropylene pyrolysis: global and mechanistic models, Energy Fuels 35 (8) (Apr. 2021) 6765–6775, https://doi.org/10.1021/acs.energyfuels.1c00342.

[99] B.A. Perez, H.E. Toraman, Investigating primary decomposition of polypropylene through detailed compositional analysis using two-dimensional gas chromatography and principal component analysis, J. Anal. Appl. Pyrolysis 177 (2024) 106376, https://doi.org/10.1016/j.jaap.2024.106376.
[100] T.M. Kruse, H.-W. Wong, L.J. Broadbelt, Mechanistic modeling of polymer pyrolysis: polypropylene, Macromolecules 36 (25) (Dec. 2003) 9594–9607, https://doi.org/10.1021/ma030322y.
[101] International Organization of Motor Vehicle Manufacturers, World Wide Fuel Charter: Gasoline and Diesel, sixth ed., 2019.